Blöcher, G., Reinsch, T., Henninges, J., Milsch, H., Regenspurg, S., Kummerow, J., Francke, H., Kranz, S., Saadat, A., Zimmermann, G., Huenges, E. (2016): Hydraulic history and current state of the deep geothermal reservoir Groß Schönebeck. - *Geothermics*, *63*, pp. 27—43.

DOI: http://doi.org/10.1016/j.geothermics.2015.07.008

Hydraulic history and current state of the deep geothermal reservoir Groß Schönebeck

Guido Blöcher[a,*], Thomas Reinsch[a], Jan Henninges[a], Harald Milsch[a], Simona Regenspurg[a], Juliane Kummerow[a], Henning Francke[a], Stefan Kranz[a], Ali Saadat[a], Günter Zimmermann[a], Ernst Huenges[a]

[a] *GFZ German Research Centre for Geosciences, Telgrafenberg, 14473 Potsdam, Germany*

Abstract

This study addresses the thermal-hydraulic-mechanical and chemical (THMC) behaviour of a research well doublet consisting of the injection well E GrSk 3/90 and the production well Gt GrSk 4/05 A(2) in the deep geothermal reservoir of Groß Schönebeck (north of Berlin, Germany). The reservoir is located between 3815 and 4247 m below sea level in the Lower Permian of the North German Basin (NGB).

Both wells were hydraulically stimulated to enhance productivity. For the production well three stimulation treatments were performed in 2007: these three treatments result in a productivity increase from 2.4 $m^3/(hMPa)$ to 14.7 $m^3/(hMPa)$. The injection well was stimulated four times in 2002/2003, resulting in a corresponding productivity increase from 0.97 $m^3/(hMPa)$ to 7.5 $m^3/(hMPa)$.

The necessary infrastructure for production and subsequent injection of geothermal fluid was established in June 2011. Between June 8, 2011

*Corresponding author
Email address: `Guido.Bloecher@gfz-potsdam.de` (Guido Blöcher)

and November 8, 2013, 139 individual hydraulic tests were performed with produced/injected volumes ranging from 4.4 to 2567 m^3. The productivity index decreased non-linearly from 8.9 $m^3/(hMPa)$ on June 8, 2011 to 0.6 $m^3/(hMPa)$ on November 8, 2013. Five possible reasons for the productivity decrease are discussed: wellbore fill, wellbore skin, the sustainability of induced fractures, two phase flow and compartmentalisation. For all hydraulic tests, the injectivity index remains almost constant at 4.0 $m^3/(hMPa)$. During 17 of 139 hydraulic tests a sudden increase of the productivity was observed. Possible reasons for this effect are discussed: accumulation of free gas and/or fines and scales within the fracture as well as changing hydraulic properties due to changing mechanical load on the fracture.

Keywords: geothermal energy, hydraulic fracturing, hydraulic test, Groß Schönebeck

1. Introduction

Geothermal energy can play an important role within the future energy supply (Sims et al., 2007), but the capability to access these resources depends on specific reservoir conditions. In high-enthalpy systems, direct use or conversion of extracted heat to electricity can be obtained at economically feasible costs. These resources are limited in most countries. Nonetheless there still exists enough heat in place in other environments to cover the heat demand for centuries. However, the initial productivity of the latter systems is often too low for an economically viable utilization without well stimulation. The efficient use of such systems is subject of current research and is covered under the technical term Enhanced or Engineered Geothermal

Systems (EGS) (e.g. Tester et al., 2006).

As a test site (Figure 1) for the provision of geothermal energy from a deep sedimentary basin in Germany, the research site at Groß Schönebeck located in the North German Basin has been developed. The site consists of a geothermal well doublet to access the sedimentary and volcanic layers of the Lower Permian (Rotliegend). The reservoir rocks are classified into two units: siliciclastic rocks (Upper Rotliegend) ranging from conglomerates (Havel subgroup) to fine-grained sandstones, siltstones and mudstones (Elbe subgroup), and volcanic rocks (Lower Rotliegend).

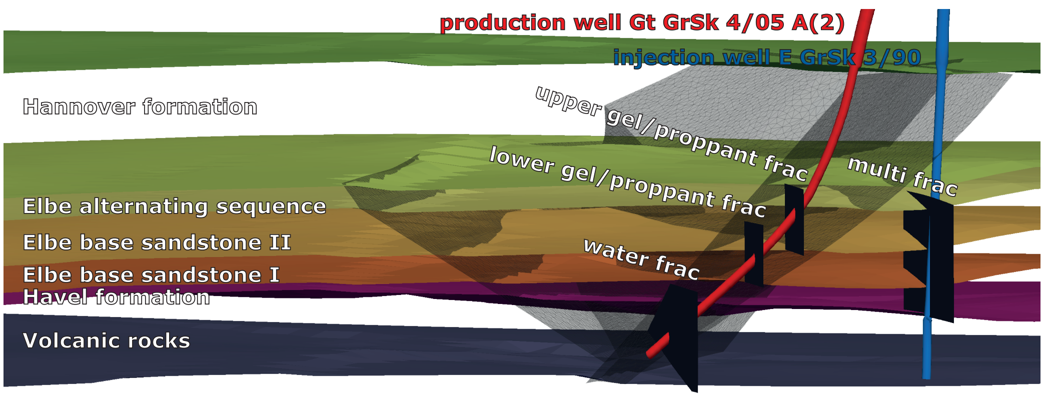

Figure 1: Schematic of the Groß Schönebeck site including major geological units, fault zones, induced hydraulic fractures as well as production well Gt GrSk 4/05 A(2) and injection well E GrSk 3/90.

The target reservoir rocks are located at a depth of 3830 to 4250 m with a temperature of 150°C (Zimmermann et al., 2011). The formation fluid contains high amounts of dissolved solids with mostly calcium, sodium and cloride as the major ions. Total amount of dissolved solids is 265 g/L (Wolfgramm et al., 2003).

An abandoned gas exploration well E GrSk 3/90 serves as injection well. The original gas exploration well with a depth of 4240 m was reopened and hydraulically tested in 2001. The test indicated a productivity index (PI) of 0.97 $m^3/(hMPa)$. Afterwards, the well was deepened to 4309 m and stimulated in 2002 and 2003 (Legarth et al., 2003, 2005). The hydraulic treatment created a NE-SW trending sub-vertical fracture in the direction of the maximum horizontal stress (N18°E +/- 3.7°) (Holl et al., 2005; Moeck et al., 2009) with a fracture half length of 160 m and a fracture height of 96 m according to the fracture simulation. A flow back test after the stimulation treatment in 2003 indicated an improvement of the PI to 7.5 $m^3/(hMPa)$, being highly sensitive to formation pressure (Zimmermann et al., 2009). A chronological sequence of all hydraulic treatments performed in the injection well E GrSk 3/90 and the corresponding change of productivity can be found in Table 1 and Table 2, respectively.

The second well Gt GrSk 4/05 A(2) was drilled as a geothermal production well in 2006. It reached a final depth of 4404.4 m with a deviation of up to 48° at bottom, where it is 475 m apart from the injection well. The initial PI of the volcanic and sandstone layers was 2.4 $m^3/(hMPa)$ (Zimmermann et al., 2010). In 2007 three stimulation treatments were carried out in different depth intervals (Zimmermann and Reinicke, 2010; Zimmermann et al., 2010). As a consequence, the initial PI was improved by a factor of 4.25 to 10.1 $m^3/(hMPa)$. A chronological sequence of all hydraulic treatments performed in the production well Gt GrSk 4/05 A(2) and the corresponding change of productivity can be found in Table 1 and Table 2, respectively.

Table 1: Chronological sequence of all induced hydraulic fractures including treatment parameters, fracture dimensions and corresponding references (1 - Legarth et al. (2003), 2 - Legarth et al. (2005), 3 - Zimmermann et al. (2009), 4 - Zimmermann et al. (2010), 5 - Zimmermann and Reinicke (2010), 6 - Zimmermann et al. (2011), 7 - Blöcher et al. (2010)) in the injection well E GrSk 3/90 and the production well Gt GrSk 4/05 A(2).

Well		**E GrSk 3/90**						**Gt GrSk 4/05 A(2)**		
Treatment		initial frac	first gel/ proppant frac	second frac	second gel/ proppant frac	first water frac	second water frac	water frac	first gel/ proppant frac	second gel/ proppant frac
Date & time										
Year		2002	2002	2002	2002	2003	2003	2007	2007	2007
Duration	$[h]$	1.9	9.3	1.7	9.5	96	67	106.5	1.5	2
Treatment parameter										
Frac interval	[MD]	4140-4200	4140-4200	4088-4128	4088-4128	3883-4294	4135-4305	4350-4404	4204-4208	4118-4122
Completion		open hole	open hole	open hole	open hole	open hole	slotted liner	slotted liner	perforated liner	perforated liner
Maximum flow rate	$[m^3/h]$	153 (stepwise)	138	121 (stepwise)	120	86.4	144	540	240	210
Cumulative volume	$[m^3]$	129	107	103	120	4284	7291	13170	280	310
Maximum well Head pressure	$[MPa]$	54.6	45.2	50.3	44.9	22	25	58.6	35	40
Gel type		HTU[1] / brine	HTU[1] / brine	HTU[1] / brine	HTU[1] / brine	-	-	-	cross-linked	cross-linked
Proppant type		-	Carbo-Lt	-	Carbo-Lt	-	-	quartz sand	high strength	high strength
Proppant mesh size		-	2040	-	2040	-	-	2040	2040	2040
Proppant mass	$[kg]$	-	8796	-	8580	-	-	24400	95000	113000
Fracture dimension										
Half length	$[m]$	-	32	-	-	-	160	190	57	60
Height	$[m]$	-	72	-	-	-	96	135	115	95
Aperture	$[cm]$	-	0.16	-	-	-	0.5	0.8	0.53	0.53
References		1,2	1,2	1,2	1,2	3	3	4	5,6	6,7

[1] cationic, hydrophilic and polymer based gel

Table 2: Chronological sequence of well tests including hydraulic parameters, reservoir performance, productivity enhancement ratio (PER) and corresponding references (1 - Zimmermann et al. (2009), 2 - Zimmermann et al. (2010), 3 - Legarth et al. (2003), 4 - Legarth et al. (2005), 5 - Zimmermann et al. (2011)) in the injection well E GrSk 3/90 and the production well Gt GrSk 4/05 A(2).

Well		**E GrSk 3/90**					**Gt GrSk 4/05 A(2)**		
well test		casing lift	casing lift	casing lift	flow back	flow back	injection	casing lift	casing lift
Date & time									
Year		2001	2002	2002	2003	2003	2007	2007	2009
Relative time		before initial frac	after first gel/proppant frac	after second gel/proppant frac	after first water frac	after second water frac	before water frac	after hydraulic treatments	after acidizing
Duration	$[h]$	12.24	8	13.92	5.76	24	13.4	11.8	4
Well test parameter									
Flow rate	$[m^3/h]$	13.5	14.8	22.4	59	35.8	31.6[2]	30.2	35
Cumulative volume	$[m^3]$	167	100	307	338	859	424[3]	356	140
Pressure difference	$[MPa]$	14	7.5	10.5	14.7	6.7	13.3	3.5	2.8
Reservoir performance									
PI/II	$[m^3/h * MPa]$	0.97	2	2.1	4	7.5	2.4	10.1	14.7
PER		initial	2.1	2.2	4.1	7.7	initial	4.3	6.2
References		1,2	3,4	1,2	1,2	1,2	2	2	5

[2] average of three single tests in different depths

[3] sum of three single tests in different depths

In 2009 a matrix acidisation treatment was performed in well Gt GrSk 4/05 A(2) using a coiled tubing unit to remove residual drilling mud in the near wellbore environment. In total 10 m^3 of 7.5 % hydrochloric acid were placed into the perforated intervals for 30 minutes and then flushed out (Zimmermann et al., 2011). A casing lift test demonstrated a further increase of productivity by 30 to 50 % to a PI between 13 to 15 $m^3/(hMPa)$.

In the framework of core screening by EEG (1990), core samples from the reservoir section in well E GrSk 3/90 were analyzed for gas permeability and porosity. The so determined permeability-depth characteristics were reproduced by Trautwein (2005) through measurements on remaining rock material. Sandstones with good reservoir quality and porosities in excess of 10% and permeabilities ranging from 5 to 100 mD at ambient conditions originate from the lower layers of the Elbe-subgroup. The transitional layers from the Elbe to the Havel-subgroup are characterized by strongly varying sedimentation conditions, porosities (ϕ = 3 to 18 %), and permeabilities (k = 0.05 to 100 mD). Apart from the upper 8 m, the sedimentary rocks of the Havel-subgroup have porosities and permeabilities ranging from 3 to 8 % and 0.001 to 0.1 mD, respectively. The andesitic volcanites of the Lower Rotliegend show porosities and permeabilities around 5 % and less than 0.01 mD, respectively.

Trautwein (2005), in addition, selected four samples from depths between 4180 to 4207 m and performed water permeability measurements under in situ pressure conditions at ambient temperature. Derived permeabilities were consistently one order of magnitude lower than those measured by EEG (1990). During drilling of well Gt GrSk 4/05 A(2), no rock coring was performed. Subsequent investigations on rock transport properties and the effects of fluid-rock interactions were performed on Rotliegend analog material from a neighboring well at Eberswalde, Germany (Eb 2/76) (Milsch et al., 2009) or from the Flechtingen quarry, Germany (Schepers and Milsch, 2013a,b). The purpose of these investigations was to constrain processes that reduce permeability during production and/or injection of fluids. Several long-term flow-through experiments were conducted under simulated in situ reservoir conditions and with durations of up to six months. No significant permeability change was observed indicating that for the type of rock present within the sandstone section of the Groß Schönebeck reservoir, damage by fines migration, clay swelling, and dissolution-precipitation reactions can be excluded under laboratory conditions.

In 2010, production well Gt GrSk 4/05 A(2) was complemented with a 4.5” production string down to 1200 m. The production string was equipped with a Y-tool having an electric submersible pump (ESP) bypassing a 2 7/8” monitoring tubing to allow for wellbore measurements during production (Figure 2). A pressure and temperature gauge was installed below the pump to monitor changes in pressure and temperature.

The necessary infrastructure for production and subsequent injection of geothermal fluid was established in June 2011. Until November 8, 2013, 139 hydraulic tests, with durations from ranging from more than 1 h to 165 h were performed. The corresponding produced volume of the individual hydraulic tests varied from less than 4.4 to 2567 m^3. During all of the discharge tests, a cumulative volume of 18900 m^3 was produced from the reservoir. Including the injection of approximately 4800 m^3 acidized fresh water in September

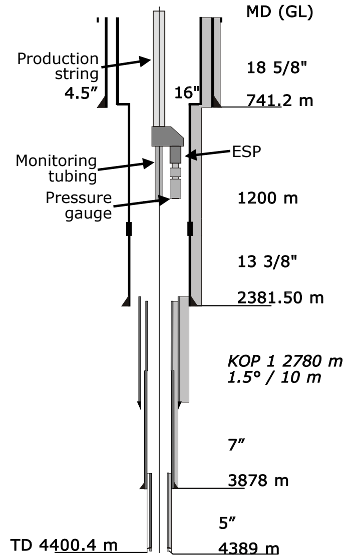

Figure 2: A schematic of the completion of the production well Gt GrSk 4/05 A(2) (modified from Reinsch et al., 2015c)

and October 2012, the cumulative injected volume during this period was about 23700 m^3 (Figure 3).

During the test period, a change in the accessible depth of the well Gt GrSk 4/05 A(2) was observed during successive logging campaigns (Regenspurg et al., 2015a) due to the precipitation of copper, barite and laurionite minerals. In order to clean out the precipitates from the production well, a coiled tubing (CT) operation was initiated in December 2012. At first, an attempt was made to clean out the well using reverse circulation through the CT. Due to the size and rheology of the solids, however, this operation failed (a detailed analysis can be found in Reinsch et al., 2015c). Therefore, a workover rig was used to clean the well in January/February 2014 (Reinsch et al., 2015b).

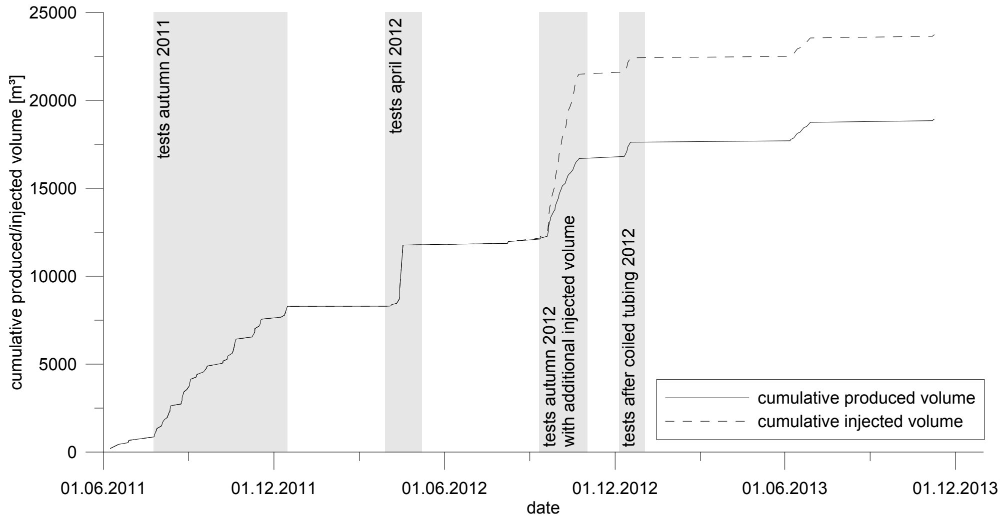

Figure 3: Cumulative produced and injected volume between June 8, 2011 and November 8, 2013.

In this paper, we present the hydraulic history of the production and the injection well. Processes influencing the productivity and injectivity of both wells will be analyzed and discussed.

2. Methods

Analyses of the 139 hydraulic tests include: test duration t, produced liquid volume from the reservoir Q_R, produced liquid volume measured at the well head Q, injected liquid volume at the well head Q_{inj}, cumulative produced liquid volume $\sum Q$, cumulative injected liquid volume $\sum Q_{inj}$, and salt concentration of the injected brine C. All quantities are provided in Appendix I. The salt concentration C was calculated by the weighted average of the produced liquid volume and the additional acidized fresh water volume having a salt concentration of 265 g/L and 0 g/L, respectively. An online measurement of the salt concentration of the injected liquid was not performed. Furthermore, all recorded data and derived quantities from the Groß Schönebeck research platform between June 8, 2011 and November 8, 2013 are available as a scientific technical report (STR) (Reinsch et al., 2015a).

The ESP was designed for a PI of approximately 6 $m^3/(hMPa)$ and the design discharge rate was 60 m^3/h with a pressure drawdown of 10 MPa in the annulus of the production well. The ESP is equipped with a variable speed drive. Reducing the pump speed results in a lower flow rate and a reduced drawdown. Since the actual PI was $\sim$1 $m^3/(hMPa)$ the pump had to maintain a pressure drawdown of 10 MPa at a flow rate of 10 m^3/h. This operating point is outside the operating range of the pump and, therefore, caused the pump to stop several times.

2.1. Production Well

For analyzing the productivity of the well, the pressure reading at the inlet of the electric submersible pump (ESP) at 1200 m depth was used (Figure 2). The pressure drawdown during production corresponds to the difference between the initial pressure $p_{ini} = 117$ bar and the pressure during production p_{dis}, both measured below the ESP. The measured fluid flow rate at the surface Q is a superposition of the flow rate generated from the reservoir Q_R and an additional contribution from the annulus Q_A. From the pressure drawdown together with the geometric information about the annulus and an assumption about the fluid density within the annulus, the contribution from the annulus can be calculated. The diameter of the production casing decreases from 16” to 13 3/8” at a depth of 741.2 m. During production, the water level within the annulus fell below this value. The change in diameter could be identified in the pressure drawdown as a change in slope when plotted versus time. The corresponding height of the water column above the ESP and its hydrostatic pressure was used to calculate the actual density of the annular fluid. From the annular flow rate and the flow rate measurement at the surface, the fluid flow rate from the reservoir was derived.

The transmissibility T of a reservoir, defined as the product of permeability and effective height of a reservoir $T = kh$, can be calculated according to Lee (1982) from the following formula, which describes the pressure buildup after shut in of the well:

$$\frac{\partial(\Delta p)}{\partial(ln\frac{t}{t+t_p})} = \frac{Q_R\mu}{4\pi kh} \tag{1}$$

where Q_R is the flow rate from the reservoir [m^3/s], μ is the dynamic viscosity [Pa s] of the fluid, k is the reservoir permeability [m^2], h its effective height [m], Δp the reservoir pressure [Pa], t is the shut-in time [s], and t_p is the production time [s].

For a doublet system (production well and injection well), with a distance d between the wells, the following formula can be applied if radial flow behavior and homogeneous reservoir conditions can be assumed (Lee, 1982):

$$PI = \frac{Q_R}{p_{ini} - p_{dis}} = \frac{2\pi T}{\mu}\frac{1}{ln(\frac{d}{r_w}) + s} \tag{2}$$

where PI is the productivity index, p_{dis} is the pressure at the production well, r_w is the well radius and s is the skin.

At the Groß Schönebeck site, hydraulic tests have been performed to test the feasibility of a continuous operation. At the beginning of the experiments, the operation was stopped after a few hours due to problems with the automatic control system on site. After adapting the control system to the hydraulic situation of the well doublet, 139 hydraulic tests with a duration of more than 1 hour could be performed and analysed. The average hydraulic test lasted a few hours with a maximum duration of about one week in April 2012. The main reason for interrupting the individual tests was the unexpected large pressure drawdown within the production well. None of the production tests reached steady state conditions. It was, therefore, decided to analyse the dynamic evolution of the productivity index. The dynamic productivity index (PI_{dyn}) was calculated as a 30 min average according to:

$$PI_{dyn} = \frac{Q}{p_{ini} - p_{dis}} \tag{3}$$

where Q is the measured flow rate at the wellhead and p_{ini} and p_{dis} are the initial and the discharge pressure at the ESP, respectively. The 30 min average of each individual test was the interval between 40 min and 10 min before test end (Figure 4). The PI_{dyn} for each test is given in Appendix I. During 17 fluid hydraulic tests a sudden change of PI_{dyn} during production was observed. To quantify this sudden productivity change a 10 min interval before and after was analysed and averaged (Figure 4).

During two hydraulic experiments, two production logging campaigns were performed in September 2011 (Henninges et al., 2012). On September 8, distributed temperature sensing (DTS) measurements were performed. From the observed temperature changes during a 2.5 h production period

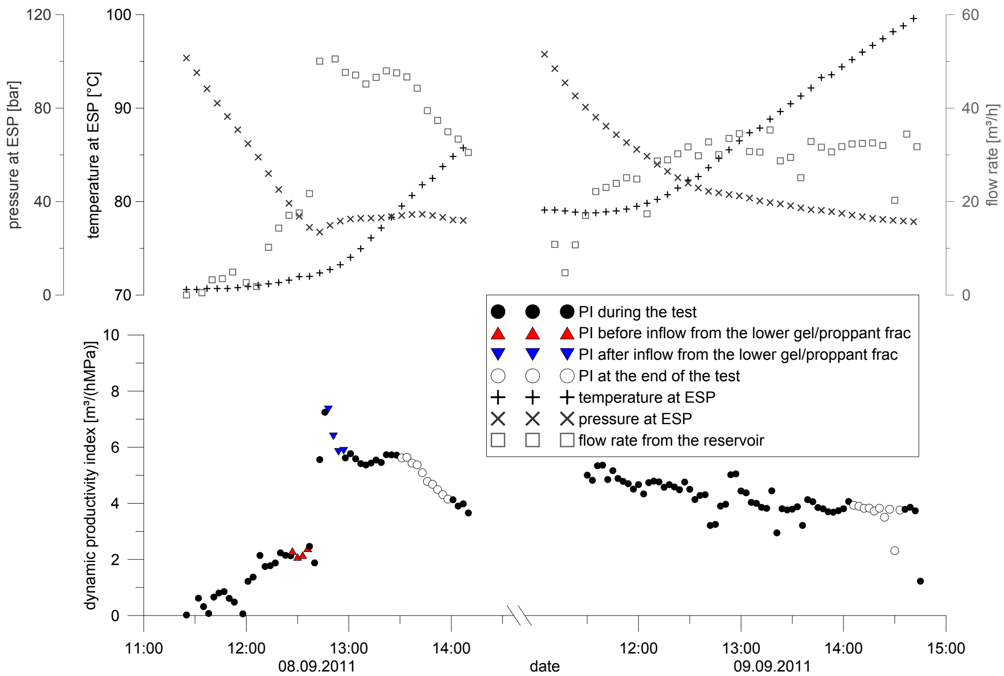

Figure 4: Measured temperature and pressure at the ESP and calculated flow rate from the reservoir with corresponding dynamic productivity index (PI_{dyn}) of the production test on September 8, 2011.

with an average fluid flow rate of 45.3 m^3/h, the fluid contribution from the lower gel/proppant frac was calculated. This calculation is based on mass and energy balance assuming constant liquid specific heat capacity (Grant, 2013).

On September 9, in addition to the DTS measurements, a p/T gauge was operated together with a spinner log during a 4 h production test with an average flow rate of 40.5 m^3/h. A detailed description of the logging campaign can be found in Henninges et al. (2012).

2.2. Injection Well

For the injection well, pressure and flow rate were measured at the wellhead during injection. In order to analyse the injectivity of the well E GrSk 3/90, the dynamic injectivity index (II_{dyn}) of the last 30 min of each hydraulic test was calculated in accordance to Equation 4 using the initial pressure p_{ini} and recharge pressure p_{rec} measured at wellhead. The II_{dyn} for each test is given in Appendix I.

$$II_{dyn} = \frac{Q}{|p_{ini} - p_{rec}|} \tag{4}$$

In order to show that the measured injectivity index depends on viscosity changes only, a numerical simulation was performed. First, the wellbore simulator by Francke (2014) was applied to calculate the trend of fluid temperature and pressure in the injection well at reservoir depth. The injection flow rate and temperature, which were continuously measured at the wellhead, were used as input parameter for the simulation. The wellbore simulator combines a compositional brine model with quasistatic thermo-hydraulic flow and radially symmetric transient conductive heat flow into the formation. In a second step, the calculated temperature of the injected fluid served as input to a 3D numerical thermo-hydraulic model of the reservoir similar to Blöcher et al. (2010), which calculates the distribution of pressure and temperature considering the temperature dependence of viscosity. Finally, the injectivity index II^{calc}_{dyn} could be calculated according to Equation 4 from the simulated injected flowrate and the calculated pressure build-up. The II^{calc}_{dyn} for each test is given in Appendix I.

3. Results

3.1. Production well

During production a non-linear reduction of the productivity from 8.9 $m^3/(hMPa)$ on June 8, 2011 to 0.6 $m^3/(hMPa)$ on November 8, 2013 was observed (Figure 5). No steady state conditions were achieved during individual tests. This means that the pressure was still decreasing at the end of each test resulting in a decreasing PI_{dyn}. This effect is best shown by the results of the hydraulic experiments in April 2012. In less than 2 weeks more than 3000 m^3 of geothermal fluid were produced during three hydraulic tests with two short tests preceding a test with a duration of one week. The PI_{dyn} computed from these three tests is significantly lower than the general trend. In addition to a decline in productivity, mineral precipitation was observed in the production well (Regenspurg et al., 2015a).

3.2. Sudden change in PI_{dyn}

Within the first six month of testing, a sudden increase of the PI_{dyn} was observed during 17 hydraulic tests (Figure 6). Production logging results from a fibre optic distributed temperature sensing survey in September 2011 (Henninges et al. (2012); Figure 7) indicate a change in fluid contribution from the lower gel/proppant frac (Figure 1). The middle panel in Figure 7 indicates that there was a contribution from the lowermost interval of the reservoir (>4355 m) at the beginning of the test, only. The contribution is indicated by colder temperatures propagating up the well with time. The relatively colder temperatures are due to the massive hydraulic stimulation within this interval. After about 2.5 h of logging, there is a sudden change

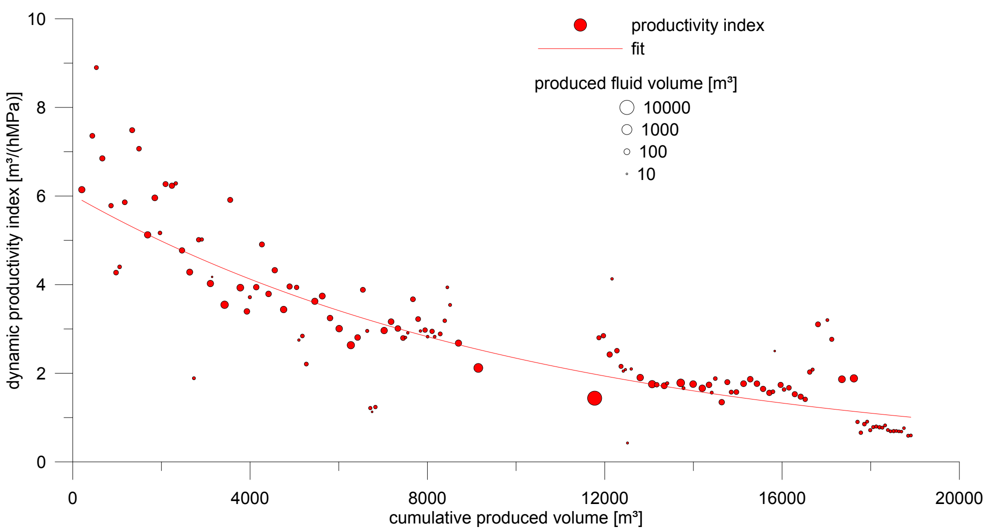

Figure 5: Dynamic productivity index (PI_{dyn}) of 139 hydraulic tests measured between June 8, 2011 and November 8, 2013.

in temperature at a depth of about 4200 m. The observed temperature increase can be explained by a changing inflow from the lower gel/proppant frac. The contribution of the lower gel/proppant frac was almost zero at the beginning of the test and changed to about 70 % at the end. Simultaneously, an increased PI_{dyn} was observed. Such a sudden increase of the PI_{dyn} was observed mostly for tests with a longer shut-in period before production as indicated at about 118, 144, 172 and 174 h of ESP operation (Figure 8). For such tests, the PI_{dyn} started at a very low level before increasing abruptly. Furthermore, it was observed that the PI_{dyn} for tests with a shorter shut-in period before production had a similar value to the value observed at the end of the previous test. For each individual test, a slight decrease of the PI_{dyn} was observed. Hydraulic data from successive tests show a slowly decreasing PI_{dyn}. A clear correlation between the amount of gas extracted at the degasser and the sudden increase of production was not observed. For some tests, however, there are indications of such a correlation. A sudden increase in production was observed at about 120 h of operation as shown in Figure 8. After an additional produced volume of 87 m^3 an increase in gas flow rate (composition of N_2 (85 - 90%) and CH_4 (10 - 15%) as published by Regenspurg et al. (2010)) at the degasser was observed. Furthermore, the amount of gas separated for the tests at 172 and 175 h showed slightly higher values compared to the tests prior to and after these tests. After the first six months this sudden increase in PI_{dyn} was no longer observed.

3.3. Injection well

In September/October 2012, 4700 m^3 of geothermal fluid was produced. After mixing this fluid with additional acidized fresh water it was injected into the injection well. Including the volume of acidized fresh water (4800 m^3), 9500 m^3 were injected. This additional acidized fresh water volume was injected in order to increase the reservoir pressure and to improve the performance of the production well. This effect was not observed by the measured PI_{dyn} as well as the subsequent shut-in pressures.

The measured II_{dyn} shows a slight decrease with cumulative injected volume. Figure 9 shows the evolution of the II_{dyn} as well as a calculated value based on a numerical approach (Section 2.2). The more volume was injected, the lower was the temperature in the near wellbore area result-

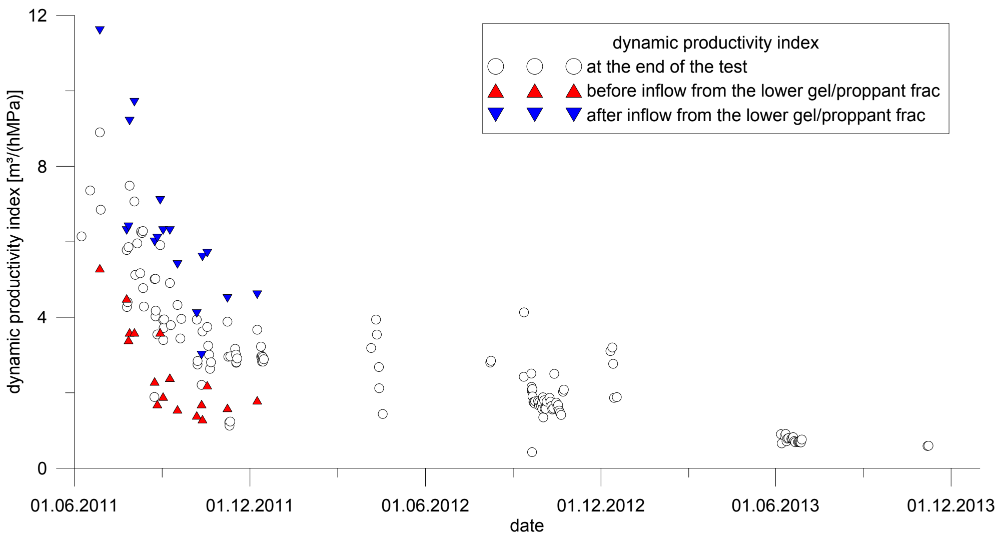

Figure 6: Dynamic productivity index (PI_{dyn}) of tests with a duration of more than 90 min and a produced volume of more than 100 m^3 each. Data of the last 30 min of each test were analyzed. Also shown is the PI_{dyn} (10 min mean) before and after opening of the lower gel/proppant frac.

ing in an increased fluid viscosity. The temperature decrease was simulated and validated by field measurements performed after the testing period by temperature logging. The increased fluid viscosity led to a decrease of the reservoir injectivity. For the injection well, no wellbore scaling was observed.

The first 54 hydraulic tests showed a range between 2.8 and 5.7 m^3/(hMPa) for the II_{dyn}. During this time no stable testing conditions were achieved. Therefore, the change of the II_{dyn} is due to variable testing condition. Afterwards, the injectivity increases to a level between 4.1 and 4.9 m^3/(hMPa).

Due to the injection of more than 3000 m^3 geothermal fluid in April 2012, the reservoir temperature was lowered, resulting in an increase in viscosity

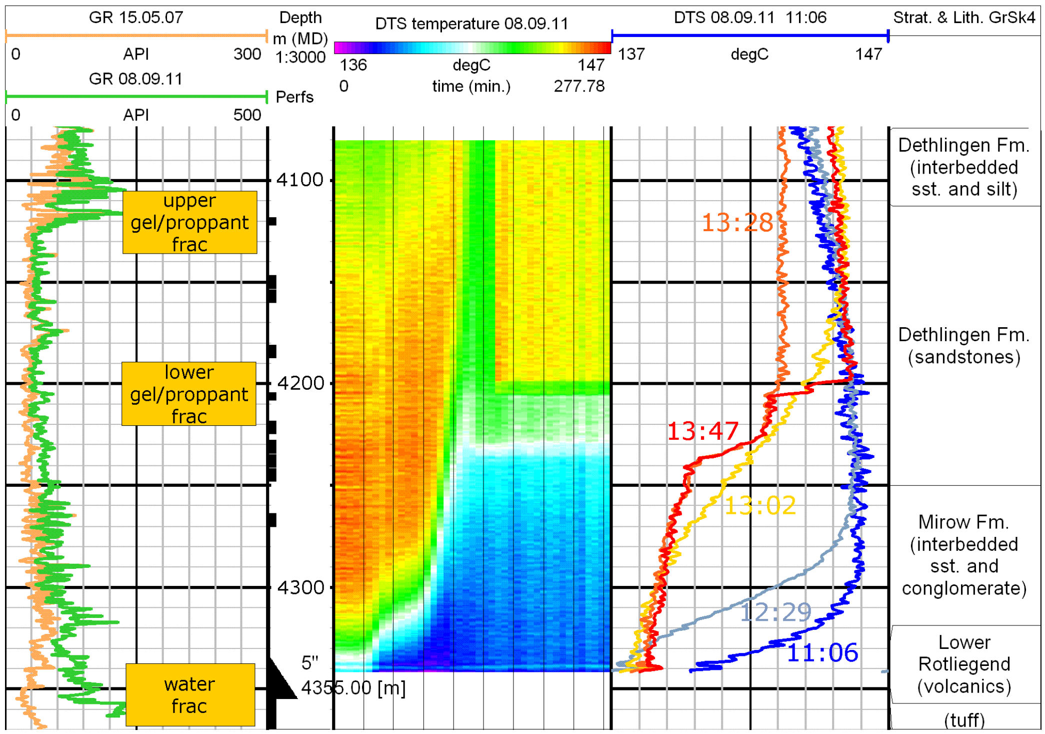

Figure 7: Gamma ray log and DTS temperature data of the production test on September 8, 2011.

and a decrease of injectivity.

4. Discussion

During the 139 hydraulic experiments between June 8, 2011 and November 8, 2013, three major observations were made: a) the decline of the productivity, and b) the sudden change of the PI_{dyn} during individual tests in the production well, as well as c) a constant injectivity in the injection well.

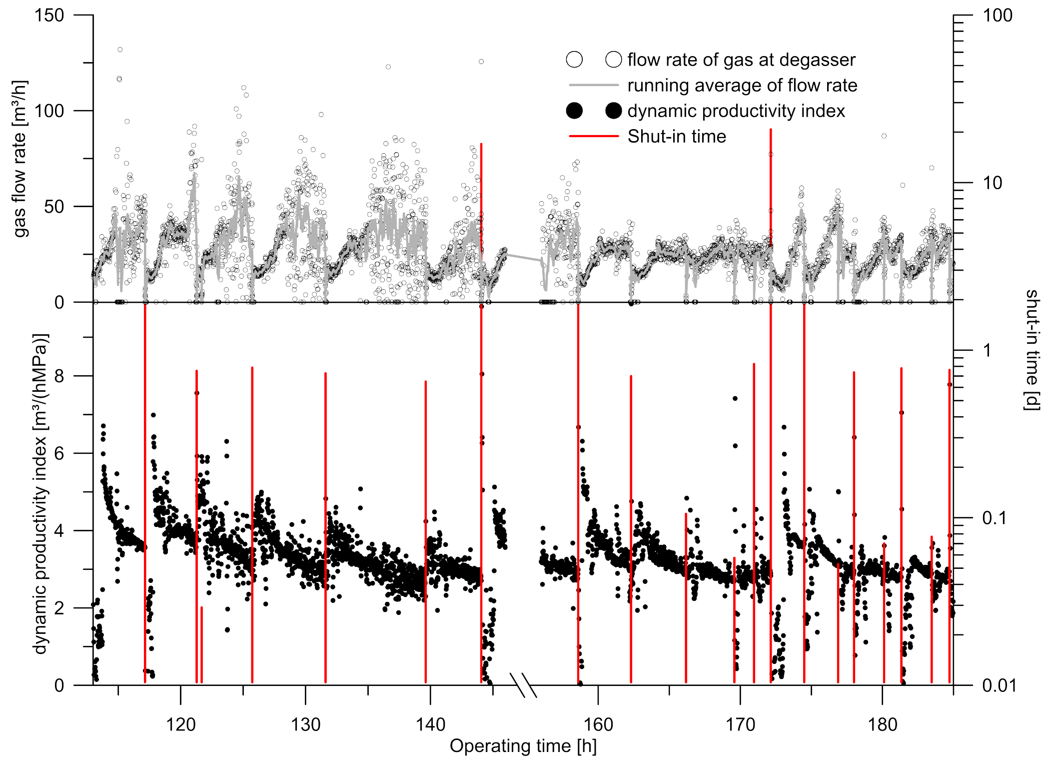

Figure 8: Dynamic productivity index (PI_{dyn}) for successive hydraulic tests together with associated shut-in times between individual tests. On the x-axis, the approximate operational time for the ESP is displayed. The panel on top shows the calculated gas flow rate from the degasser.

4.1. Production well

The decline of the productivity cannot be explained by a single process. Minerals clogging the well, wellbore skin due to copper precipitation, change in the hydraulic properties of the stimulated fractures, two-phase flow and hydraulic barriers in the reservoir are possible candidates for the overall productivity decline and are discussed in the following.

The abrupt variations in the PI_{dyn} are most likely linked to a changing

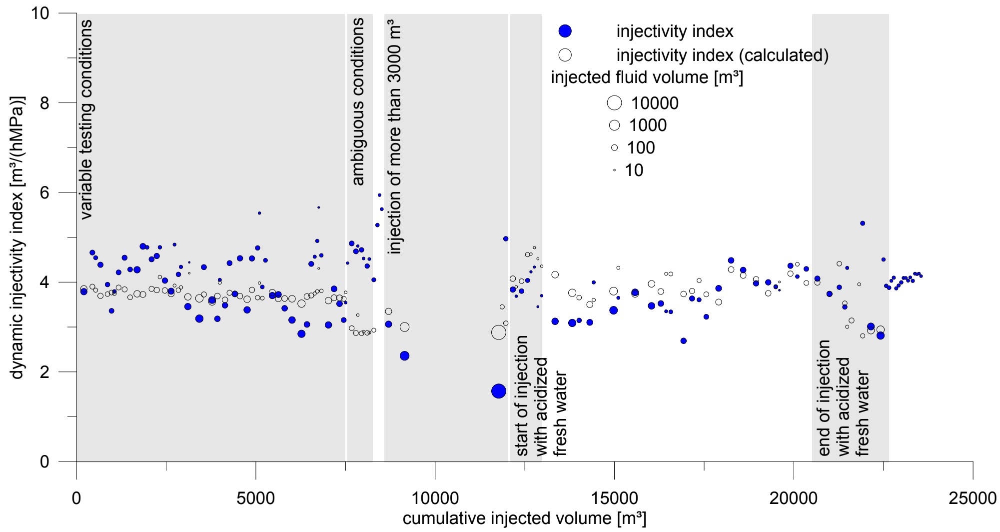

Figure 9: Dynamic injectivity index (II_{dyn}) of 139 hydraulic tests measured between June 8, 2011 and November 8, 2013.

influx from the lower gel/proppant frac. These sudden changes were observed during 17 hydraulic tests and were investigated by temperature profiling in September 2011. The sudden change of the PI_{dyn} occurred mostly after longer shut-in periods. The processes which lead to this behaviour are discussed in the following.

4.1.1. Productivity decline

Wellbore fill. Measurements of the total wireline accessible depth performed during several logging campaigns between 2010 and 2012 showed a decrease in accessible depth over time from 4360 to 4116 m. The collection of bailer samples revealed that the changing depth was caused by minerals clogging the well. Two wellbore clean out operations removed large amounts of the fill to a final depth of 4345 m in January/February 2014. The material collected from filters, bailer, and clean out operations was analyzed and quantified (Regenspurg et al., 2015a). It was found that it consists solely of minerals and amorphous phases that formed by direct precipitation indicating that no solid material from the reservoir had entered the wellbore. The identified minerals were native copper (Cu; 18 %), barite (Sr,$BaSO_4$; 28 %); laurionite (PbOHCl) and amorphous lead phases (9 %), calcite ($CaCO_3$; 6 %), magnetite (Fe_3O_4, 20 %) and unidentified amorphous phases (15 %) consisting of a mixture of Si, Al, Fe and Ca as well as about 5 % organic carbon.

The formation of the minerals happened either due to cooling of the brine during shut-in (barite), slight shifts of the pH (laurionite), or due to electrochemical reactions of Cu-bearing formation fluid with the steel casing resulting in precipitation of native copper and magnetite. Altogether about 600 L of solid material are estimated to have been removed from the well (by coiled tubing, clean out and filtering during plant operation).

It seems likely, that the fill is responsible for the decreased production rate. However, laboratory test of the fill material revealed high permeability values between 0.57 and 2.7 D (Meißner, 2014). This was confirmed by a lift test, performed after the well clean out down to 4345 m that showed only little increase in the production rate thus demonstrating that the fill in the uppermost part of the reservoir interval was not hydraulically tight. However, since the composition of the material was not homogeneous along the well and the material density increased with increasing depth, it cannot be ruled out completely that the clogging material below 4345 m (within the fractured area of the volcanic rocks) has lower hydraulic conductivity. Nevertheless, other processes seem more likely to be responsible for the productivity decline in the sandstone layers.

Wellbore skin. The occurrence of high amounts of dissolved copper in the geothermal brine is typical for Rotliegend formations (Blundell et al., 2003; Cathles et al., 1993; Hitzman et al., 2010). In these highly saline waters, chloride prevents Cu saturation by formation of aqueous Cu(II) or Cu(I) chloride complexes. However, the introduction of carbon steel with a more negative electric potential ($Fe_0 \rightarrow Fe^{2+} + 2e^-$; E_0 = -0.44 V) than Cu ($Cu^{2+} + 2e^- \rightarrow Cu_0$; E_0 = 0.34 V) results in reduction of Cu(II) to Cu(0) that precipitates (Figure 10). This reaction most likely happens on both, inside and outside of the casing. While the precipitates of Cu within the well can be removed, sampled and quantified, it only can be assumed that the same process happens on the outside of the casing as well. This kind of precipitation would increasingly clog the pores of the nearby reservoir resulting in a positive wellbore skin. In a laboratory study, this process was simulated showing complete reduction of the pore space around and at some distance from a steel pipe (Regenspurg et al., 2015b). In contrast, the negative skin values obtained during the hydraulic tests (Appendix II, Table 4) indicate a high conductivity connection between the wellbore and the reservoir through the induced fractures.

Sustainability of induced fractures. Hydraulically induced fractures provide enhanced permeability in enhanced geothermal systems. However, the lifespan of hydraulically induced fractures is limited in time by chemical and mechanical effects. These effects strongly depend on changes in pressure and

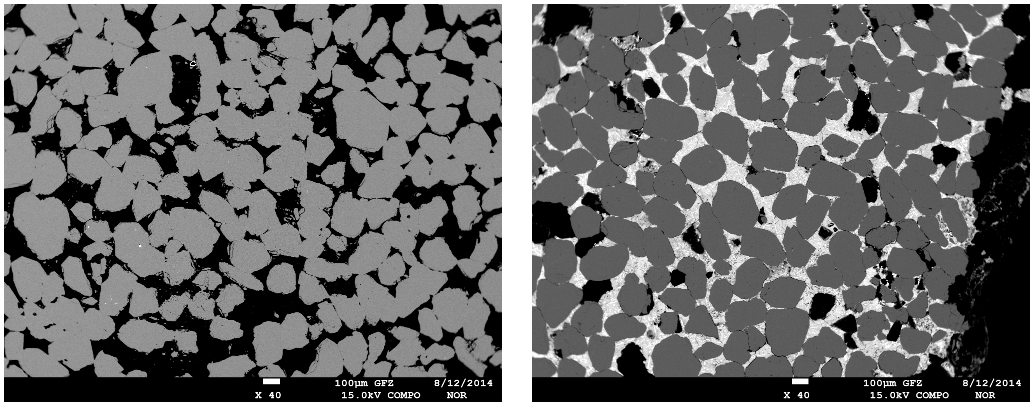

(a) (b)

Figure 10: Electron microprobe picture of sandstone samples (with integrated carbon steel tube; not shown) before (a) and after (b) flow through with a copper (1 mM) chloride solution at anoxic conditions. Pores spaces are shown in black, quartz grains in grey, and pore space filling with copper and iron oxides in white.

temperature, stability of proppants, fluid-rock interactions, fracture morphology and the stress state.

During stimulation treatments in well Gt GrSk 4/05 A(2) induced quartz sand (volcanic section) and high strength proppants (sandstone section) were used to keep the fractures open during production (Table 1) as well as to achieve a longer life time of the system (Zimmermann and Reinicke, 2010; Zimmermann et al., 2010). The stability of the high strength proppants was tested under simulated in situ pressure and temperature conditions in the laboratory (Zimmermann and Reinicke, 2010; Deon et al., 2013). The permeability of the rock-proppant system stabilised after some time and there was no expectation of a long-term effect related to the mechanical interactions between the proppants and the fracture faces under constant drawdown conditions. Under in situ temperature conditions some changes in the proppant stability could be observed (Deon et al., 2013). However, in contrast to the latter observation, proppants recovered after being in the well for several years did not show any damage (Zimmermann et al., 2014).

In addition to the stability of the proppants, mineral alteration by dissolution and precipitation as well as mechanical effects (e.g. grain crushing, brecciation, compaction and mineral replacement) can induce formation damage (Reinicke et al., 2012; Kneafsey et al., 2015). Therefore, the sustainability of the induced hydraulic fractures at Groß Schönebeck is questionable. The stress state in the enhanced geothermal system was altered during the 139 hydraulic tests. During several hydraulic tests, the reservoir pressure was greatly reduced to provide maximum test duration. For some individual tests this drawdown reached values of approximately 10 MPa. Due the reduction of reservoir pressure the effective stresses on the hydraulic fractures are increased by the same amount. How these alternating stress changes effect the sustainability of the induced fractures is still unknown but the changes of the PI_{dyn} and of the overall productivity indicate a negative influence.

Two-phase flow. Downhole fluid sampling data indicate a free gas phase during production. Existence of two fluid phases (e.g. brine and gas) in a porous medium is known to significantly affect its hydraulic properties (e.g. Abaci et al., 1992, and references therein). Two-phase flow through porous rocks reduces the effective permeabilities of the individual fluid phases, because a part of the pore volume is occupied by one fluid phase and thus the effective pore volume available for the flow of the other fluid is reduced.

To assess the effect of partial gas saturation on the productivity of the

Groß Schönebeck reservoir, effective permeabilities, k_{eff}, were measured on a sandstone sample having a permeability $k_{sat} = 116$ mD. This sample were taken from the lower part of the Elbe-subgroup (well E GrSk 3/90). The core sample was saturated with synthetic brine (2 M NaCl + 0.5 M $CaCl_2$) and was subsequently flooded parallel to the sample axis. After applying a constant differential pressure, Δp, the fluid flow rate, Q, was determined. The permeability was calculated from the Darcy equation:

$$k = \frac{Q \cdot l \cdot \mu}{\Delta p} \cdot \frac{1}{\pi r^2}, \tag{5}$$

where r and l are radius and length of the sample, and μ is the dynamic viscosity of the pore fluid. The flooding was performed at different levels of partial sample saturation. To obtain decreasing brine saturation, N_2 was successively injected into the sample. The corresponding sample saturation, S_W, was derived from the pore volume of the sample and the brine volume produced from the sample. After each drainage step, the sample was percolated with brine again to obtain the flow rate at partial saturation. The relative permeability, k_{rel}, at a certain saturation level is given by the effective permeability, k_{eff}, normalized by the permeability k_{sat} of the completely brine saturated sample:

$$k_{rel} = \frac{k_{eff}}{k_{sat}}. \tag{6}$$

Results are shown in Figure 11. A strong dependence between k_{rel} and S_W was observed for the investigated sample. k_{rel} decreases exponentially with increasing partial saturation. The data show that 3 % of free gas phase in the rock causes a reduction in relative permeability of about 25 %. At a gas saturation of 20 %, k_{rel} is reduced to about 20 % of its initial value and decreases with further increasing gas saturation ($S_W = 45$ %) to $k_{rel} = 12$ %.

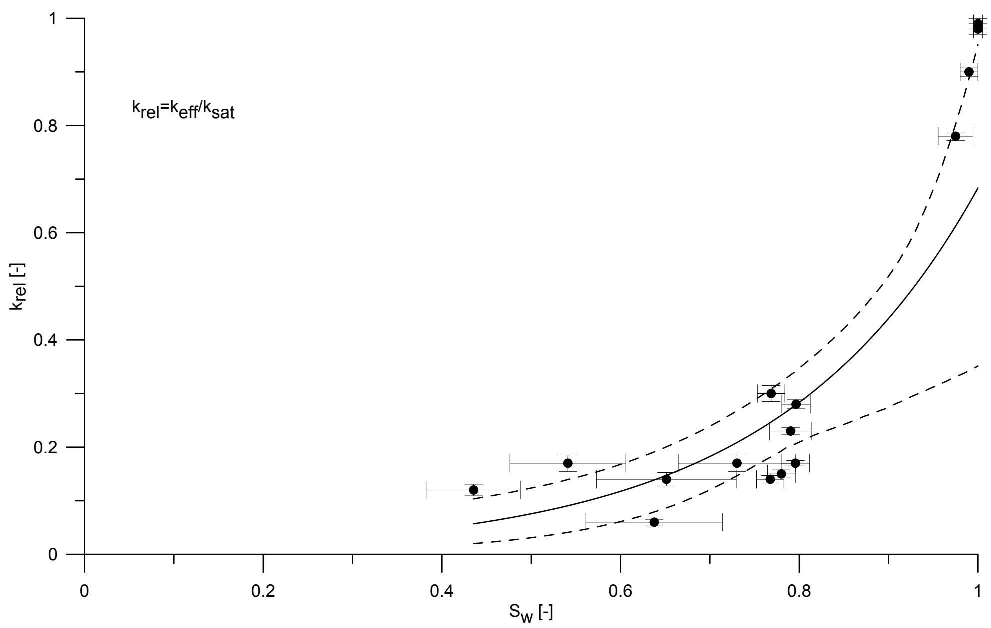

Figure 11: Relative permeability k_{rel} of a sandstone sample from the Groß Schönebeck reservoir as function of brine saturation. Scatter values and large error bars reflect the influence of re-saturation during the flooding of the partially saturated sample. The data is fitted by an exponential function. Dashed lines show the 95 % confidence interval.

The extent to which a cyclic operation of the production well with corresponding fluid pressure changes will trigger the development of a free gas phase in the Groß Schönebeck reservoir, is not fully understood yet. However, a number of fluid samples suggest that the saturation of the formation fluid with CH_4 and N_2 is at least close to their solubility limits. This means that, when lowering the reservoir pressure during production, the solubility limit is exceeded, and could lead to degassing of the formation fluid and the expansion of a free gas phase. This might cause a decrease in the effective permeability of the formation and thus a decrease in productivity of the hydraulic system.

Hydraulic Barriers - Compartmentalisation. Several hydraulic test were performed in September/October 2011 with production periods of approximately one day. Curve matching of the final pressure build up according to standard well testing analysis (Horne, 1995) showed a radial symmetric flow regime and a no-flow boundary (hydraulic barrier) on one side of the reservoir at a distance of approximately 330 m. A continuous hydraulic test in April 2012 with a test duration of 7 days showed similar results. Again, the pressure build up was investigated and pressure matching yielded a radial symmetric flow regime with a no-flow boundary (hydraulic barrier) at a distance of approximately 122 m. Furthermore, the productivity of the well declined from 2.4 $m^3/(hMPa)$ in September/October 2011 to 1.5 $m^3/(hMPa)$ in April 2012 based on transmissibility and skin calculation and assuming pseudo-radial flow according to Lee (1982). Pressure matching of several hydraulic tests in September/October 2012 again showed a radial symmetric response with a no-flow boundary at a distance of 670 m. The corresponding transmissibility, skin and productivity index were $8.2 \cdot 10^{-14}$ m^3, -5.6 and 1.9 m^3 /(hMPa). respectively. A detailed description of the well test analysis can be found in Appendix II. The existence of a similar no-flow boundary at the injection well could not be shown by additional well test analysis.

Since the pressure data, especially the derivative plot, gave no indication for a bilinear or linear flow (Cinco-Ley and Samaniego-V., 1981), the production data were analyzed by type curve matching assuming pseudo-radial flow. Due to short production time the produced volume from the reservoir Q_R (about 100 m^3, see Table 3) is smaller than the estimated total fracture volume of 540 m^3. Therefore, the pressure responses reflect the hydraulic behavior of the fracture system and the near wellbore region. The changing distance of the no-flow boundary can, therefore, be interpreted as a change of the hydraulically assessable area due to changing reservoir conditions with time.

4.1.2. Sudden change in PI_{dyn}

The sudden change of the productivity can be related to a changing contribution from the lower gel/proppant frac. The reasons for the changing contribution are largely unknown. Possible reasons are:

1. Accumulation of gas in the fracture leading to a reduction of the permeability for liquid brine. A changing contribution might be accounted for by a sudden reduction of the accumulated amount of gas. An indication for this process might be a higher amount of gas produced in tests where a changing contribution was observed.
2. Accumulation of fines/scales in the fracture during longer shut-in periods. A changing contribution might be accounted for by a production of these fines into the well due to the increasing differential pressure. Such fines would either be produced to the surface or they would accumulate in the lower part of the well.
3. Changing hydraulic properties due to changes in mechanical load on the fracture surfaces during longer shut-in periods.

Accumulation of gas in the fracture. The changing contribution from the lower gel/proppant frac does not show a significant correlation with the calculated gas flow rate from the degasser. The produced volume for each test, where a changing contribution was observed, is smaller than the wellbore storage volume (215 m^3 for total water column). Thus, it is possible that the fluid entering the well during individual tests did not reach the surface during the same test. For the test at about 120 h of operating time, about 87 m^3 of fluid were produced from the reservoir between the change in the PI_{dyn} and the change in gas flow rate at the degasser. A clear answer on the amount of gas being released during different tests cannot be given. Therefore, the question whether an accumulation of gas in the gel/proppant frac might reduce the permeability for liquid geothermal brine cannot be fully answered.

Accumulation of fines/scales in the fracture. An increasing amount of fines in the produced geothermal brine was observed in the first tests after a longer shut-in period. These precipitates, however, were mostly observed at the very beginning of tests, indicating a precipitation due to the cooling of the liquid brine within the wellbore. A changing accessible depth of the well was observed, too. The changing depth, however, was mostly observed after the first 6 months of production, where a change in PI_{dyn} was not observed anymore. Thus, a direct correlation between the change in PI_{dyn} and the accumulation of fines in individual tests cannot be inferred.

Change in mechanical load. During individual hydraulic tests the fluid pressure was decreased by up to 10 MPa within the reservoir resulting in an increase of effective pressure. This increase of effective pressure should yield a decrease in fracture aperture and, therefore, permeability. This effect could not be validated by the observations. Therefore, a sudden change in the fracture conductivity as a response to an effective pressure variation is questionable.

4.2. Injection well

Due to the injection of 4800 m^3 acidized fresh water in September/October 2012, the temperature in the injection zone of the reservoir and the salinity of the injected fluid were reduced. A reduction of temperature increases the fluid viscosity whereas the reduced salt concentration decreases the fluid viscosity. Based on available temperature and salt concentration data, the salinity effects is assumed to be dominant. The measured data confirm that the injection of acidized fresh water increases the II_{dyn}. In December 2012 the injection of acidized fresh water was stopped and the II_{dyn} decreased due to an increase of salt concentration and viscosity, accordingly.

Between December 2012 and June 2013 no further hydraulic experiments were performed. In June 2013 the measured II_{dyn} show a relative increase. This indicates an increase of the reservoir temperature and a reduction of viscosity during the shut-in period.

The general behaviour of the described effects was interpreted as a change in fluid viscosity due to temperature, salt concentration and pressure changes. The performed 3D numerical simulation (Section 2.2), considering density and viscosity changes, explains and validates these results.

4.3. Reservoir Pressure

The performance of a reservoir in terms of productivity or injectivity index should be quantified according to the flow rate and pressure changes in the reservoir. However, in most cases pressure and flow rate are measured at the surface (wellhead) and are therefore influenced by the transient characteristics of the water column in the well. Therefore, if transient effects like temperature changes of the injected/produced fluids in the column cannot be neglected, wellhead pressures must be corrected to compute reservoir pressures. The same is valid for the flow rate since the reservoir flow is retarded at the beginning of a hydraulic test. Temperature variations cause changes in the density of the fluid column and hence lead to transient buoyancy effects. Furthermore, viscosity of the fluid is temperature dependent and influences injectivity index of the injection well. Since the inlet temperature of the production well is almost constant, the viscosity effect must be considered for the production wellbore, only. In case absolute values are needed a correction is mandatory. If relative changes in pressure are sufficient for a correct interpretation of reservoir performance, a correction is not necessarily needed but potential inconsistencies especially at the beginning of hydraulic tests have to be addressed.

5. Conclusions

During production a non-linear reduction of the productivity index from 8.9 $m^3/(hMPa)$ on June 8, 2011 to 0.6 $m^3/(hMPa)$ on November 8, 2013 was observed. Within the first six month of testing, a sudden increase of the PI_{dyn} was observed during 17 hydraulic tests.

The transient behaviour of the productivity index is non-linear and indicates an irreversible change of the reservoir characteristics. The reduction of the productivity index might be explained by an accumulation of scale within the wellbore, non-sustainable hydraulically induced fractures and a decrease of reservoir permeability due to scaling or two-phase flow. Furthermore, a compartmentalisation might cause the productivity decrease. The variation of the injectivity index can be explained by a change of fluid viscosity and fluid density within the reservoir due to injection of colder water with variable salt concentration. These transient effects change the frictional pressure loss inside the reservoir and lead to a changing injectivity.

The sudden increase of productivity is due to activation of the lower gel/proppant frac. The contribution from the latter fracture increases after sufficiently long shut-in periods before production. The abrupt inflow from the lower gel/proppant frac might be explained by two-phase flow and corresponding relative permeabilities as well as by the accumulation of fines/scales in the fracture or by an effective pressure dependence (mechanical effect) of the induced fracture conductivity. The exact reason, however, remains unknown.

The decline of the overall productivity cannot be explained by a single process. However, for each single process technical approaches exist which can improve the performance of the deep geothermal reservoir of Groß Schönebeck. Minerals clogging in the well can be reduced by a proper completion material which reduces the electro-chemical reactions of the fluid with the casing. The long term precipitation and sedimentation of minerals can be avoided by a constant production temperature and high flow rates. Wellbore skin due to copper precipitation can be avoided by the use of materials which reduce electro-chemical reactions between fluid, rock and well casing. Degassing of the produced fluid can be reduced by a lower pressure drawdown during production. Furthermore, the reduced pressure drawdown will prolong the mechanical sustainability of the induced fractures.

6. Acknowledgements

This work has been performed in the framework of the two projects ”sustainable production and injection of thermal water from the deep sedimentary reservoir of Groß Schönebeck” [BMU, FKZ0325088] and ”qualification of geothermal technologies, integration of subsurface and surface facilities” [BMU, FKZ0325217], which were funded by the German Federal Ministry for the Environment, Nature Conservation and Nuclear Safety. The work on mineral precipitation of the wellbore fill was funded by the German Federal Ministry of Energy and Economics (BMWi) and the German Federal Ministry of Environment, Nature Conversation and Nuclear Safety within the framework of the project ”Langzeit-Korrosionsuntersuchungen und -Monitoring in salinarem Thermalwasser” [BMWi/BMU, FKZ0325069A]. The authors would like to thank two anonymous reviewers and the guest editor Sabodh Garg for significantly improving the manuscript.

7. References

Abaci, S., Edwards, J., Whittaker, B., 1992. Relative permeability measurements for two phase flow in unconsolidated sands. Mine Water and the

Environment 11 (2), 11–26.
URL http://dx.doi.org/10.1007/BF02919583

Blöcher, M. G., Zimmermann, G., Moeck, I., Brandt, W., Hassanzadegan, A., Magri, F., 2010. 3D numerical modeling of hydrothermal processes during the lifetime of a deep geothermal reservoir. Geofluids 10 (3), 406–421.
URL http://dx.doi.org/10.1111/j.1468-8123.2010.00284.x

Blundell, D. J., Karnkowski, P. H., Alderton, D. H. M., Oszczepalski, S., Kucha, H., 2003. Copper mineralization of the polish Kupferschiefer: a proposed basement fault-fracture system of fluid flow. Economic Geology and the Bulletin of the Society of Economic Geologists 97 (7), 1487–1495.
URL http://dx.doi.org/10.2113/gsecongeo.98.7.1487

Cathles, L. M., Oszczepalski, S., Jowett, E. C., 1993. Mass balance evaluation of the late diagenetic hypothesis for Kupferschiefer Cu mineralization in the Lubin Basin of southwestern Poland. Economic Geology and the Bulletin of the Society of Economic Geologists 88 (4), 948–956.
URL http://dx.doi.org/10.2113/gsecongeo.88.4.948

Cinco-Ley, H., Samaniego-V., F., 1981. Transient pressure analysis for fractured wells. Journal of Petroleum Technology 33 (9), 1749 – 1766.

Deon, F., Regenspurg, S., Zimmermann, G., 2013. Geochemical interactions of Al_2O_3-based proppants with highly saline geothermal brines at simulated in situ temperature conditions. Geothermics 47 (0), 53 – 60.

EEG, 1990. drilling report. Tech. rep., EEG-Erdgas Erdöl GmbH.

Francke, H., 2014. Thermo-hydraulic model of the two-phase flow in the brine circuit of a geothermal power plant. Ph.D. thesis, TU Berlin.
URL urn:nbn:de:kobv:83-opus4-47126

Grant, M., 2013. Geothermal Reservoir Engineering. Energy science and engineering. Elsevier Science.

Henninges, J., Brandt, W., Erbas, K., Moeck, I., Saadat, A., Reinsch, T., Zimmermann, G., 2012. Downhole monitoring during hydraulic experiments at the in-situ geothermal lab Gross Schönebeck. In: Proceedings 37th Workshop on Geothermal Reservoir Engineering. No. 194 in SGP-TR. Stanford, USA, pp. 51–56.

Hitzman, M. W., Selley, D., Bull, S., 2010. Formation of sedimentary rock-hosted stratiform copper deposits through Earth history. Economic Geology and the Bulletin of the Society of Economic Geologists 105 (3), 627–639.
URL http://dx.doi.org/10.2113/gsecongeo.105.3.627

Holl, H., Moeck, I., Schandelmeier, H., 2005. Characterisation of the tectono-sedimentary evolution of a geothermal reservoir - implications for exploitation (southern permian basin, ne germany). In: Proceedings World Geothermal Congress 2005 Antalya, Turkey, 24-29 April 2005. p. 5.

Horne, R. N. (Ed.), 1995. Modern Well Test Analysis: A Computer-Aided Approach, 2nd Edition. Petro Way.

Kneafsey, T. J., Nakagawa, S., Dobson, P. F., Kennedy, B. M., 2015. Fracture Sustainability in EGS Systems Results of Laboratory Studies. In:

Fourtieth Workshop on Geothermal Reservoir Engineering Stanford University, Stanford, California SGP-TR-204. p. 9.

Lee, J. (Ed.), 1982. Well Testing. Vol. SPE textbook series vol. 1. Society of Petroleum Engineers.

Legarth, B., Huenges, E., Zimmermann, G., 2005. Hydraulic fracturing in a sedimentary geothermal reservoir: Results and implications. International Journal of Rock Mechanics and Mining Sciences 42 (78), 1028 – 1041, rock Physics and Geomechanics Rock Physics and Geomechanics.
URL http://dx.doi.org/10.1016/j.ijrmms.2005.05.014

Legarth, B., Tischner, T., Huenges, E., 2003. Stimulation experiments in sedimentary, low-enthalpy reservoirs for geothermal power generation, Germany. Geothermics 32 (46), 487 – 495, selected Papers from the European Geothermal Conference 2003.
URL http://dx.doi.org/10.1016/j.geothermics.2003.07.007

Meißner, M., 2014. Bestimmung des kf-Wertes unter anaeroben Bedingungen Laborversuche mit Gestein aus einer geothermischen Tiefbohrung. Bachelor Thesis, Technische Universität Berlin.

Milsch, H., Seibt, A., Spangenberg, E., 2009. Long-term petrophysical investigations on geothermal reservoir rocks at simulated in situ conditions. Transport in Porous Media 77 (1), 59–78.
URL http://dx.doi.org/10.1007/s11242-008-9261-5

Moeck, I., Schandelmeier, H., Holl, H.-G., 2009. The stress regime in a Rotliegend reservoir of the Northeast German Basin. International Journal

of Earth Sciences 98 (7), 1643–1654.
URL http://dx.doi.org/10.1007/s00531-008-0316-1

Regenspurg, S., Feldbusch, E., Byrne, J., Deon, F., Driba, D. L., Henninges, J., Kappler, A., Naumann, R., Reinsch, T., Schubert, C., 2015a. Mineral precipitation during production of geothermal fluid from a Permian Rotliegend reservoir. Geothermics 54 (0), 122 – 135.
URL http://dx.doi.org/10.1016/j.geothermics.2015.01.003

Regenspurg, S., Milsch, H., Schaper, J., 2015b. Copper in geothermal brine: Origin, reactions, risk and chances. In: Proceedings World Geothermal Congress 2015 Melbourne, Australia, 19-24 April 2015. p. 5.

Regenspurg, S., Wiersberg, T., Brandt, W., Huenges, E., Saadat, A., Schmidt, K., Zimmermann, G., 2010. Geochemical properties of saline geothermal fluids from the in-situ geothermal laboratory Groß Schönebeck (Germany). Chemie der Erde - Geochemistry 70, Supplement 3 (0), 3 – 12.

Reinicke, A., Blöcher, G., Zimmermann, G., Huenges, E., Dresen, G., Stanchits, S., Legarth, B. A., Makurat, A., 2012. Mechanically Induced Fracture-Face Skin–Insights From Laboratory Testing and Modeling Approaches. Society of Petroleum Engineers 28 (1), 26–35.

Reinsch, T., Blöcher, G., Kranz, S., 2015a. Data From The Groß Schönebeck Research Platform 2011-06-01 - 2013-12-31. Tech. rep., Helmholtz Centre Potsdam GFZ German Research Centre for Geosciences.

Reinsch, T., Kranz, S., Saadat, A., Huenges, E., Rinke, M., Brandt, W., Schulz, P., 2015b. Managed pressure wellbore cleanout operation - optimize a reverse cleanout applying the airlift concept within a drill sting. SPE Production & Operations(submitted).

Reinsch, T., Regenspurg, S., Feldbusch, E., Saadat, A., Huenges, E., Erbas, K., Zimmermann, G., Henninges, J., 2015c. Reverse cleanout in a geothermal well: Analysis of a failed coiled-tubing operation. SPE Production & Operations Preprint (Preprint), 9.

Schepers, A., Milsch, H., 2013a. Dissolution-precipitation reactions in hydrothermal experiments with quartz-feldspar aggregates. Contributions to Mineralogy and Petrology 165 (1), 83–101.
URL http://dx.doi.org/10.1007/s00410-012-0793-x

Schepers, A., Milsch, H., 2013b. Relationships between fluid-rock interactions and the electrical conductivity of sandstones. Journal of Geophysical Research: Solid Earth 118 (7), 3304–3317.
URL http://dx.doi.org/10.1002/jgrb.50241

Sims, R., Schock, R., Adegbululgbe, A., Fenhann, J., Konstantinaviciute, I., Moomaw, W., Nimir, H., Schlamadinger, B., Torres-Martínez, J., Turner, C., Uchiyama, Y., Vuori, S., Wamukonya, N., Zhang, X., 2007. Energy supply. In: Metz, B., Davidson, O. R., Bosch, P. R., Dave, R., Meyer, L. A. (Eds.), Climate Change 2007: Mitigation. Contribution of Working Group III to the Fourth Assessment Report of the Intergovernmental Panel on Climate Change. Cambridge University Press, Cambridge, United Kingdom and New York, NY, USA, pp. 251–322.

Tester, J., Anderson, B., Batchelor, A., Blackwell, D., DiPippo, R., Drake, E., Garnish, J., Livesay, B., Moore, M., Nichols, K. M., Petty, S., Toksöz, M., Veatch, R., Baria, R., Augustine, C., Murphy, E., Negraru, P., Richards, M., 2006. The Future of Geothermal Energy: Impact of Enhanced Geothermal Systems (EGS) on the United States in the 21st century. Tech. rep., Massachusetts Institute of Technology. 0-615-13438-6.

Trautwein, U., 2005. Poroelastische Verformung und petrophysikalische Eigenschaften von Rotliegend Sandsteinen. Ph.D. thesis, Universitätsbibliothek.

Wolfgramm, M., Seibt, A., Hurter, S., Zimmermann, G., 2003. Origin of geothermal fluids of Permo-Carboniferous rocks in the NE German basin (NE Germany). Journal of Geochemical Exploration 7879 (0), 127 – 131. URL http://dx.doi.org/10.1016/S0375-6742(03)00133-X

Zimmermann, G., Blöcher, G., Reinicke, A., Brandt, W., 2011. Rock specific hydraulic fracturing and matrix acidizing to enhance a geothermal system Concepts and field results. Tectonophysics 503 (12), 146 – 154. URL http://dx.doi.org/10.1016/j.tecto.2010.09.026

Zimmermann, G., Blöcher, G., Reinicke, A., Deon, F., Regenspurg, S., Yoon, J.-S., Zang, A., Heidbach, O., Moeck, I., Huenges, E., 2014. Hydraulische Stimulationskonzepte zur Entwicklung von Enhanced Geothermal Systems (EGS). System Erde 4 (1), 30 – 35.

Zimmermann, G., Moeck, I., Blöcher, G., 2010. Cyclic waterfrac stimulation to develop an Enhanced Geothermal System (EGS)Conceptual design and experimental results. Geothermics 39 (1), 59 – 69, the European I-

GET Project: Integrated Geophysical Exploration Technologies for Deep Geothermal Reservoirs.
URL http://dx.doi.org/10.1016/j.geothermics.2009.10.003

Zimmermann, G., Reinicke, A., 2010. Hydraulic stimulation of a deep sandstone reservoir to develop an Enhanced Geothermal System: Laboratory and field experiments. Geothermics 39 (1), 70 – 77.
URL http://dx.doi.org/10.1016/j.geothermics.2009.12.003

Zimmermann, G., Tischner, T., Legarth, B., Huenges, E., 2009. Pressure-dependent production efficiency of an Enhanced Geothermal System (EGS): Stimulation results and implications for hydraulic fracture treatments. In: Vinciguerra, S., Bernab, Y. (Eds.), Rock Physics and Natural Hazards. Pageoph Topical Volumes. Birkhuser Basel, pp. 1089–1106.
URL http://dx.doi.org/10.1007/978-3-0346-0122-1_16

List of Figures

List of Tables

Appendix I: Data used for the analysis of the 139 hydraulic tests

Table 3: Selected data of the 139 hydraulic tests including: test duration t, produced volume from reservoir Q_R, produced volume measured at the well head Q, injected volume at the well head Q_{inj}, cumulative produced volume $\sum Q$, cumulative injected volume $\sum Q_{inj}$, dynamic productivity index PI_{dyn}, dynamic injectivity index II_{dyn}, calculated dynamic injectivity index II_{dyn}^{calc} and salt concentration of the injected brine C

DateTime	t	Q_R	Q	Q_{inj}	$\sum Q$	$\sum Q_{inj}$	PI_{dyn}	II_{dyn}	II_{dyn}^{calc}	C
DD:MM:YYYY hh:mm	$[h]$	$[m^3]$	$[m^3]$	$[m^3]$	$[m^3]$	$[m^3]$	$[m^3/(hMPa)]$	$[m^3/(hMPa)]$	$[m^3/(hMPa)]$	$[g/L]$
08.06.2011 09:25	4.4	141.2	189.4	189.4	204.2	204.2	6.1	3.8	3.9	265
17.06.2011 10:27	2.5	75.7	116.3	116.3	441.4	441.4	7.4	4.7	3.9	265
27.06.2011 11:12	1.9	54.3	87.4	87.4	532.7	532.7	8.9	4.5	3.8	265
28.06.2011 09:20	2.9	90	133.2	133.2	666.8	666.8	6.9	4.4	3.7	265
25.07.2011 10:43	2.4	58.3	102.2	102.2	863.1	863.1	5.8	3.9	3.7	265
25.07.2011 16:11	3.1	73.5	112.5	112.5	976.1	976.1	4.3	3.4	3.8	265
26.07.2011 10:31	1.9	36.8	79.4	79.4	1056.8	1056.8	4.4	3.8	3.7	265
27.07.2011 09:17	2.8	70	115.7	115.7	1172.8	1172.8	5.9	4.2	3.9	265
28.07.2011 12:17	2.7	80.5	124.1	124.1	1339.7	1339.7	7.5	4.5	3.8	265
02.08.2011 12:17	2.4	71.9	109.7	109.7	1493.8	1493.8	7.1	4.3	3.7	265
03.08.2011 10:22	3.9	139.1	193.7	193.7	1688.7	1688.7	5.1	4.3	3.7	265
05.08.2011 12:41	3.2	113.4	159.5	159.5	1850.6	1850.6	6	4.8	3.7	265
08.08.2011 13:43	1.7	44.3	77.9	77.9	1967.5	1967.5	5.2	4.8	ND	265
09.08.2011 09:32	2.7	83.9	125.7	125.7	2093.2	2093.2	6.3	4.5	3.9	265
10.08.2011 10:23	2.8	90.5	137.1	137.1	2236.4	2236.4	6.2	4.6	3.8	265

Table 3 Continued

DateTime	t	Q_R	Q	Q_{inj}	$\sum Q$	$\sum Q_{inj}$	PI_{dyn}	II_{dyn}	II_{dyn}^{calc}	C
DD:MM:YYYY hh:mm	$[h]$	$[m^3]$	$[m^3]$	$[m^3]$	$[m^3]$	$[m^3]$	$[m^3/(hMPa)]$	$[m^3/(hMPa)]$	$[m^3/(hMPa)]$	$[g/L]$
11.08.2011 09:45	1.5	42.5	73.6	73.6	2324.1	2324.1	6.3	4.8	4.1	265
11.08.2011 13:43	2.9	93.3	140	140	2464.1	2464.1	4.8	4	3.8	265
12.08.2011 09:53	3.9	123.2	173.3	173.3	2637.4	2637.4	4.3	3.8	3.7	265
23.08.2011 08:51	1.4	12.5	62.3	62.3	2733	2733	1.9	4.8	3.9	265
23.08.2011 14:24	2.5	69.2	102.1	102.1	2840.6	2840.6	5	4.2	3.8	265
24.08.2011 08:49	1.7	36.3	70.2	70.2	2910.8	2910.8	5	4.3	3.9	265
24.08.2011 11:51	4.9	150.6	193.6	193.6	3104.4	3104.4	4	3.5	3.7	265
24.08.2011 17:25	1	27	38.9	38.9	3143.3	3143.3	4.2	4.4	4.2	265
26.08.2011 10:12	7.1	224.9	279.2	279.2	3424.7	3424.7	3.5	3.2	3.6	265
29.08.2011 09:43	3.1	79.3	126	126	3550.8	3550.8	5.9	4.3	3.7	265
01.09.2011 10:24	5.4	167.2	222.6	222.6	3779.3	3779.3	3.9	3.6	3.6	265
01.09.2011 16:26	4.5	132	148.5	148.5	3927.8	3927.8	3.4	3.2	3.7	265
01.09.2011 23:02	1.5	37.8	66.6	66.6	3994.6	3994.6	3.7	4.1	4	265
02.09.2011 13:50	3.3	97.2	144.4	144.4	4139	4139	3.9	3.5	3.6	265
08.09.2011 11:25	2.8	75.4	123.1	123.1	4266.6	4266.6	4.9	4.4	3.8	265
09.09.2011 11:03	3.7	97.9	149.7	149.7	4416.3	4416.3	3.8	3.7	3.7	265
16.09.2011 10:18	3.1	83.7	140.3	140.3	4556.6	4556.6	4.3	4.5	3.7	265
19.09.2011 10:04	5.3	149.7	199.9	199.9	4756.5	4756.5	3.4	3.4	3.6	265

Table 3 Continued

DateTime	t	Q_R	Q	Q_{inj}	$\sum Q$	$\sum Q_{inj}$	PI_{dyn}	II_{dyn}	II_{dyn}^{calc}	C
DD:MM:YYYY hh:mm	$[h]$	$[m^3]$	$[m^3]$	$[m^3]$	$[m^3]$	$[m^3]$	$[m^3/(hMPa)]$	$[m^3/(hMPa)]$	$[m^3/(hMPa)]$	$[g/L]$
20.09.2011 11:13	3.1	78.5	134.4	134.4	4890.9	4890.9	4	4.5	3.8	265
06.10.2011 12:47	2.2	43.5	100.9	100.9	5048.9	5048.9	3.9	4.8	3.7	265
07.10.2011 07:33	1.1	11	51.6	51.6	5100.5	5100.5	2.7	5.5	4	265
07.10.2011 09:32	2	42.7	79.3	79.3	5179.9	5179.9	2.8	3.9	3.6	265
11.10.2011 13:50	1.9	23.7	83.9	83.9	5268.2	5268.2	2.2	4.5	ND	265
12.10.2011 11:27	5	132.5	187.4	187.4	5459.8	5459.8	3.6	3.7	3.8	265
17.10.2011 11:15	4.3	112.4	168	168	5627.8	5627.8	3.7	3.7	3.6	265
18.10.2011 10:33	4.2	106.2	148.6	148.6	5803.1	5803.1	3.2	3.4	3.6	265
19.10.2011 09:30	6	149.2	205.9	205.9	6009	6009	3	3.2	3.6	265
20.10.2011 08:50	8.2	207	264	264	6273	6273	2.6	2.8	3.5	265
21.10.2011 08:26	4.6	101.2	152	152	6425	6425	2.8	3.1	3.7	265
07.11.2011 12:52	2.7	61.6	119	119	6544.1	6544.1	3.9	4.4	3.7	265
08.11.2011 10:29	1.6	27.6	66.1	66.1	6641.8	6641.8	3	4.6	3.7	265
09.11.2011 09:31	1.6	7.3	70.1	70.1	6711.9	6711.9	1.2	4.9	3.8	265
09.11.2011 16:06	1.1	4.9	40.9	40.9	6752.8	6752.8	1.1	5.7	4.3	265
10.11.2011 10:19	1.7	16.3	74.2	74.2	6827	6827	1.2	4.6	3.8	265
10.11.2011 13:29	6.2	164.6	196.5	196.5	7023.5	7023.5	3	3	3.6	265
15.11.2011 12:33	3.9	98.3	157.2	157.2	7180.7	7180.7	3.2	3.9	3.7	265

Table 3 Continued

DateTime	t	Q_R	Q	Q_{inj}	$\sum Q$	$\sum Q_{inj}$	PI_{dyn}	II_{dyn}	II_{dyn}^{calc}	C
DD:MM:YYYY hh:mm	$[h]$	$[m^3]$	$[m^3]$	$[m^3]$	$[m^3]$	$[m^3]$	$[m^3/(hMPa)]$	$[m^3/(hMPa)]$	$[m^3/(hMPa)]$	$[g/L]$
16.11.2011 09:04	4	96.4	152.8	152.8	7333.5	7333.5	3	3.5	3.7	265
16.11.2011 15:28	3.6	83	117.1	117.1	7450.6	7450.6	2.8	3.2	3.6	265
16.11.2011 20:15	1.5	32.4	54.4	54.4	7505	7505	2.8	3.5	3.8	265
17.11.2011 17:29	1.3	22.7	52.8	52.8	7557.8	7557.8	2.9	4.4	ND	265
08.12.2011 13:35	2.5	55	115.4	115.4	7673.2	7673.2	3.7	4.9	3	265
12.12.2011 11:07	2.5	55.1	117.3	117.3	7790.5	7790.5	3.2	4.7	2.9	265
12.12.2011 14:46	1.3	27.7	52.8	52.8	7843.3	7843.3	3	4.8	3.3	265
13.12.2011 09:34	2.3	42.2	103.4	103.4	7946.9	7946.9	3	4.7	2.9	265
13.12.2011 13:22	1.4	27.8	57	57	8003.9	8003.9	2.8	4.5	2.9	265
14.12.2011 09:18	2.3	42.1	101.1	101.1	8105	8105	2.9	4.4	2.9	265
14.12.2011 13:17	1.4	28.4	58.6	58.6	8163.6	8163.6	2.8	4.5	2.9	265
15.12.2011 10:46	2.1	46	86.2	86.2	8288.5	8288.5	2.9	4.1	2.9	265
30.03.2012 12:02	1.4	ND	ND	ND	8296.4	8296.4	ND	ND	ND	265
02.04.2012 13:03	1.1	ND	ND	ND	8299.5	8299.5	ND	ND	ND	265
03.04.2012 11:41	1.6	ND	ND	ND	8302.9	8302.9	ND	ND	ND	265
04.04.2012 06:45	2.1	ND	12.4	12.4	8315.4	8315.4	ND	ND	ND	265
05.04.2012 07:58	1.6	24.5	75.5	75.5	8390.9	8390.9	3.2	5.3	ND	265
10.04.2012 09:05	1.2	14.6	58.5	58.5	8449.4	8449.4	3.9	5.9	ND	265

Table 3 Continued

DateTime DD:MM:YYYY hh:mm	t $[h]$	Q_R $[m^3]$	Q $[m^3]$	Q_{inj} $[m^3]$	$\sum Q$ $[m^3]$	$\sum Q_{inj}$ $[m^3]$	PI_{dyn} $[m^3/(hMPa)]$	II_{dyn} $[m^3/(hMPa)]$	II_{dyn}^{calc} $[m^3/(hMPa)]$	C $[g/L]$
11.04.2012 07:07	1.4	16.1	62.3	62.3	8511.6	8511.6	3.5	5.6	ND	265
13.04.2012 09:55	6.5	134.4	186.4	186.4	8700.7	8700.7	2.7	3.1	3.3	265
13.04.2012 16:54	23.1	427.8	447.5	447.5	9148.2	9148.2	2.1	2.4	3	265
17.04.2012 09:46	165	2567.3	2624.3	2624.3	11772.5	11772.5	1.4	1.6	2.9	265
07.08.2012 11:49	2.7	30.9	93	93	11868.5	11868.5	2.8	ND	3.4	265
08.08.2012 07:26	2.2	36.1	101.7	101.7	11970.2	11970.2	2.8	5	3.1	265
11.09.2012 10:27	4.8	86.2	136.7	190.6	12111.1	12165	2.4	3.8	4.1	192
11.09.2012 16:53	2.6	43.7	53.4	95.1	12164.7	12260.4	4.1	3.7	3.9	149
19.09.2012 08:04	3.8	54.3	107.3	146.1	12275.2	12409.9	2.5	3.8	4	196
19.09.2012 14:15	4.3	62.2	92	166.5	12367.2	12576.3	2.2	4	4.6	146
19.09.2012 19:27	2.5	34.5	51	95.1	12418.2	12671.4	2	4.2	4.6	142
19.09.2012 22:42	2.6	35.2	48.9	95.8	12467.1	12767.2	2.1	4.3	4.8	135
20.09.2012 02:03	3	36.1	46.1	96.8	12513.2	12864	0.4	3.5	4.5	126
20.09.2012 10:09	2.4	33.6	52.6	74.5	12597.5	12970.2	2.1	3.7	4.4	210
20.09.2012 13:14	11.2	183.6	202.1	373.7	12799.6	13343.9	1.9	3.1	4.2	143
21.09.2012 12:19	14.5	221	269	478.8	13068.8	13822.9	1.8	3.1	3.8	149
22.09.2012 05:34	5.7	79.2	104.5	191.7	13173.3	14014.6	1.7	3.1	3.7	145
22.09.2012 18:59	8.9	127.3	168.1	296.5	13341.7	14311.3	1.7	3.1	3.5	150

Table 3 Continued

DateTime DD:MM:YYYY hh:mm	t $[h]$	Q_R $[m^3]$	Q $[m^3]$	Q_{inj} $[m^3]$	$\sum Q$ $[m^3]$	$\sum Q_{inj}$ $[m^3]$	PI_{dyn} $[m^3/(hMPa)]$	II_{dyn} $[m^3/(hMPa)]$	II_{dyn}^{calc} $[m^3/(hMPa)]$	C $[g/L]$
23.09.2012 09:52	2.7	34	67.3	109.9	13409	14421.2	1.8	4	3.6	162
26.09.2012 09:08	16.6	245.7	304.2	553.7	13713.3	14975	1.8	3.4	3.8	146
27.09.2012 08:16	3.7	36.1	63.4	132.3	13776.8	15107.3	1.7	3.7	4.3	127
27.09.2012 18:18	11.9	169.6	217.3	467.4	13994	15574.7	1.8	3.8	3.7	123
29.09.2012 05:28	12.4	156.3	205.7	458.5	14199.9	16033.5	1.7	3.5	4	119
30.09.2012 09:01	6.7	100.5	151.5	259.6	14351.4	16293.2	1.7	3.5	3.8	155
30.09.2012 19:36	4.2	42.7	61.9	147.6	14413.5	16440.9	1.6	3.4	4.2	111
01.10.2012 10:05	3.5	41.4	80.6	130	14494.1	16571	1.9	3.3	4.2	164
01.10.2012 18:35	11	118.2	144.5	355.3	14638.7	16926.3	1.3	2.7	3.7	108
02.10.2012 16:08	6.4	78.7	126.5	237	14765.2	17163.3	1.8	3.6	3.8	141
03.10.2012 06:33	5.2	53.2	88.5	196.6	14853.7	17359.9	1.6	3.6	4	119
04.10.2012 06:06	5.7	68	115.5	200.4	14969.1	17560.3	1.6	3.2	3.7	153
05.10.2012 06:24	8.7	108.7	162.5	344.2	15131.7	17904.6	1.8	3.9	3.6	125
08.10.2012 08:54	8.3	92.6	150.5	348.1	15282.2	18252.7	1.9	4.5	4.3	115
09.10.2012 07:36	8.2	95.8	150.7	336.2	15432.9	18588.9	1.8	4.3	4.2	119
10.10.2012 06:44	8.9	90.8	139.1	359.6	15572	18948.5	1.6	4	4.1	103
11.10.2012 05:54	8.2	91.3	141.8	339	15713.8	19287.6	1.6	4	3.8	111
12.10.2012 07:27	5.3	44.8	80.5	209.2	15794.3	19496.8	1.6	3.9	3.9	102

Table 3 Continued

DateTime	t	Q_R	Q	Q_{inj}	$\sum Q$	$\sum Q_{inj}$	PI_{dyn}	II_{dyn}	II_{dyn}^{calc}	C
DD:MM:YYYY hh:mm	$[h]$	$[m^3]$	$[m^3]$	$[m^3]$	$[m^3]$	$[m^3]$	$[m^3/(hMPa)]$	$[m^3/(hMPa)]$	$[m^3/(hMPa)]$	$[g/L]$
13.10.2012 06:02	2.7	19.9	40.5	102.8	15834.8	19599.5	2.5	3.8	4	104
15.10.2012 08:06	7.2	76	132.9	307.1	15967.7	19906.6	1.7	4.4	4.2	115
16.10.2012 12:23	4.7	37	77.3	193	16045.1	20099.7	1.6	4.1	4.4	106
17.10.2012 06:58	5.8	57.7	109.9	249.8	16155	20349.5	1.7	4.3	4	117
18.10.2012 07:35	7.1	77.2	131.8	308.5	16286.8	20658	1.5	4.1	4	113
19.10.2012 06:46	8	85.5	133.2	337.3	16420.1	20995.3	1.5	3.7	3.7	105
20.10.2012 10:22	6.8	58	102.2	274.1	16522.3	21269.5	1.4	3.9	4.4	99
22.10.2012 08:19	4.1	42.4	101.3	154.2	16623.6	21423.6	2	3.4	3.5	174
23.10.2012 06:18	1.7	16.5	65.8	65.8	16689.4	21489.4	2.1	4.3	3	265
10.12.2012 18:37	2.7	45.4	120.5	120.5	16810.6	21610.6	3.1	ND	3.1	265
12.12.2012 19:12	1.5	19.4	60.5	60.5	17022.1	21822.2	3.2	ND	4	265
13.12.2012 14:28	2.1	32.7	93.9	93.9	17120.8	21920.8	2.8	5.3	2.8	265
14.12.2012 12:39	10.1	167.6	229.6	229.6	17350.3	22150.4	1.9	3	2.9	265
17.12.2012 10:37	13	213.3	269.8	269.8	17620.2	22420.2	1.9	2.8	2.9	265
06.06.2013 12:16	2.5	8.5	72.9	72.9	17702	22502.1	0.9	4.5	ND	265
07.06.2013 08:40	3.2	13.5	74.8	74.8	17776.8	22576.9	0.7	3.9	ND	265
10.06.2013 09:09	4.1	14.6	80.3	80.3	17857.1	22657.2	0.9	3.9	ND	265
11.06.2013 10:56	2.6	8.7	62.9	62.9	17920.2	22720.3	0.9	4	ND	265

Table 3 Continued

DateTime	t	Q_R	Q	Q_{inj}	$\sum Q$	$\sum Q_{inj}$	PI_{dyn}	II_{dyn}	II_{dyn}^{calc}	C
DD:MM:YYYY hh:mm	$[h]$	$[m^3]$	$[m^3]$	$[m^3]$	$[m^3]$	$[m^3]$	$[m^3/(hMPa)]$	$[m^3/(hMPa)]$	$[m^3/(hMPa)]$	$[g/L]$
12.06.2013 08:35	2.6	9.9	68.2	68.2	17988.6	22788.6	0.7	4.1	ND	265
13.06.2013 08:14	2.9	9.6	68.1	68.1	18056.7	22856.8	0.8	3.9	ND	265
14.06.2013 08:50	2.8	9.2	66.7	66.7	18123.4	22923.5	0.8	3.9	ND	265
17.06.2013 09:30	3	8.7	74	74	18197.4	22997.4	0.8	4	ND	265
18.06.2013 09:21	2.5	7.8	64.6	64.6	18262.7	23062.8	0.8	4.1	ND	265
19.06.2013 07:35	2.4	6.9	61.3	61.3	18324	23124	0.8	4.1	ND	265
20.06.2013 10:05	2.5	6.3	63.1	63.1	18387.1	23187.2	0.7	4	ND	265
21.06.2013 09:18	2.3	6.8	60	60	18447.2	23247.3	0.7	4.1	ND	265
24.06.2013 08:57	2.7	6.4	70.9	70.9	18518.1	23318.2	0.7	4	ND	265
25.06.2013 09:41	2.3	5.6	59.8	59.8	18578.1	23378.2	0.7	4.2	ND	265
26.06.2013 09:32	2.3	5.2	58.2	58.2	18636.3	23436.3	0.7	4.2	ND	265
27.06.2013 08:26	2.1	4.4	56	56	18692.2	23492.3	0.7	4.2	ND	265
28.06.2013 07:31	2.2	5.6	57.2	57.2	18749.5	23549.6	0.8	4.1	ND	265
06.11.2013 07:54	2.6	5.2	65.3	65.3	18845.4	23645.5	0.6	ND	ND	265
07.11.2013 09:11	2.5	4.9	59.9	59.9	18905.4	23705.5	0.6	ND	ND	265
08.11.2013 09:08	1.1	ND	22	22	18927.6	23727.6	ND	ND	ND	265

Appendix II: Detailed analysis of hydraulic tests

The recovery phase of three different hydraulic tests were analysed, which are characterised by an extended time of production and a subsequent shut-in phase.

September/October 2011 test

The hydraulic test in September/October 2011 was performed in several cycles of production of approximately one day each. Figure 12 shows the progression of the whole test and the final shut-in period used for well test analysis.

Standard curve matching analysis (e.g. Horne, 1995) showed a radial symmetric flow regime and a no-flow boundary on one side of the reservoir at a distance of 330 m (Figure 13).

Curve matching yielded a transmissibility of $1.24 \cdot 10^{-13}$ m^3. The corresponding skin is -5.2 and implies a good connection of the induced fractures to the well. From these values the productivity index is calculated as 2.4 m^3 /(hMPa). For a doublet with an effective distance between the two wells of 300 m the corresponding productivity index is 2.1 m^3 /(hMPa).

April 2012 test

The hydraulic test in April 2012 was the first test with continuous flow for 7 days. After production the well was shut-in to record the pressure build up (Figures 14 and 15).

Pressure matching yielded a radial symmetric flow regime and a no-flow boundary at a distance of 122 m. Transmissibility was calculated as $1.14 \cdot 10^{-13}$ m^3 and skin amounts to -3.7 again indicating a good connection of the

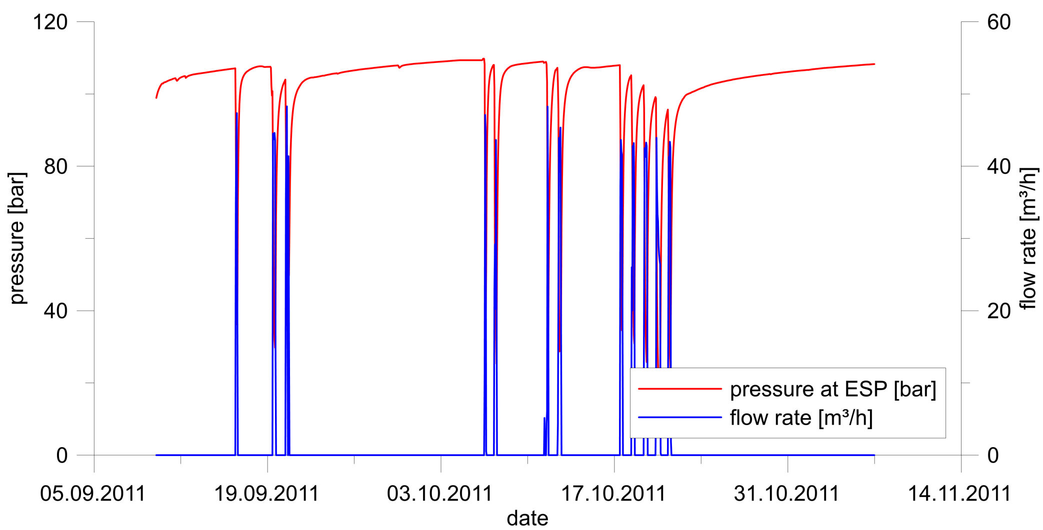

Figure 12: Progression of the hydraulic tests from September/October 2011.

fractures to the well. From these values the productivity index was calculated as 1.5 m^3 /(hMPa). For a doublet with an effective distance of the two wells of 300 m the corresponding productivity index is 1.4 m^3 /(hMPa).

September/October 2012 test including additional injection

During the hydraulic tests in September/October 2012 in addition to the produced formation fluid acidized fresh water was injected. In total 4800 m^3 of additional acidized fresh water were injected. Pressure matching again yielded a radial symmetric response with a no-flow boundary at a distance of 670 m. The corresponding transmissibility and the skin were $8.2 \cdot 10^{-14}$ m^3 and -5.6, respectively. From these values the resulting productivity index, 1.9 m^3 /(hMPa) is similar to the results of the test in April 2012 and for the doublet solution 1.6 m^3 /(hMPa) (Figures 16 and 17).

A summary of all test results can be found in Table 4.

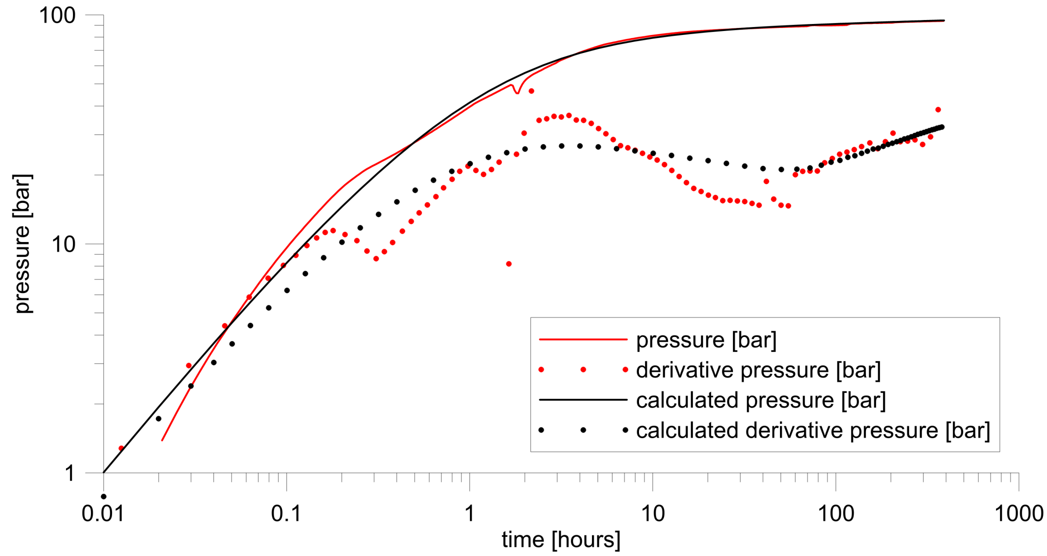

Figure 13: Curve matching of pressure build up during the final shut-in period and its derivative function of the hydraulic test from September /October 2011.

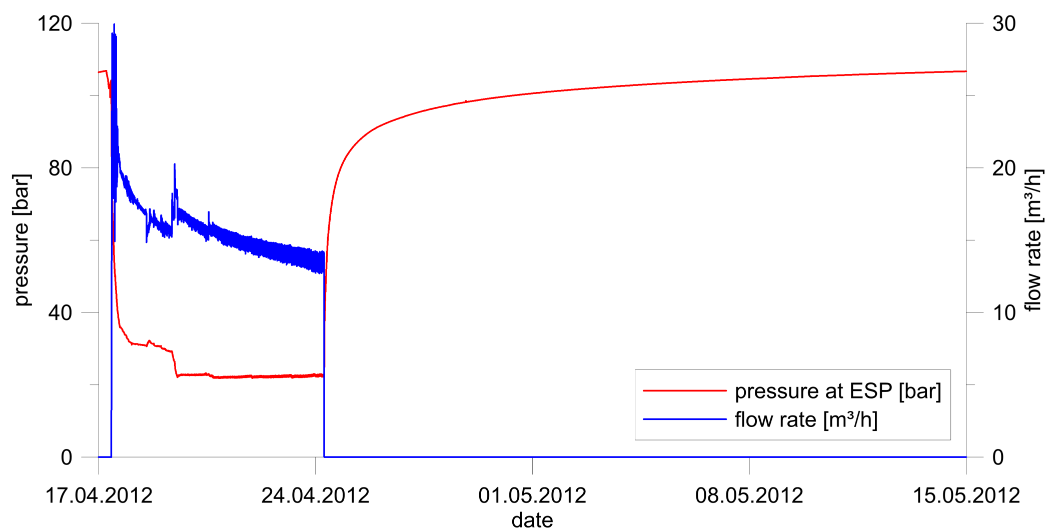

Figure 14: Progression of the hydraulic tests from April 2012. Displayed are the flow rate and the pressure at the electrical submersible pump installed at 1200 m depth.

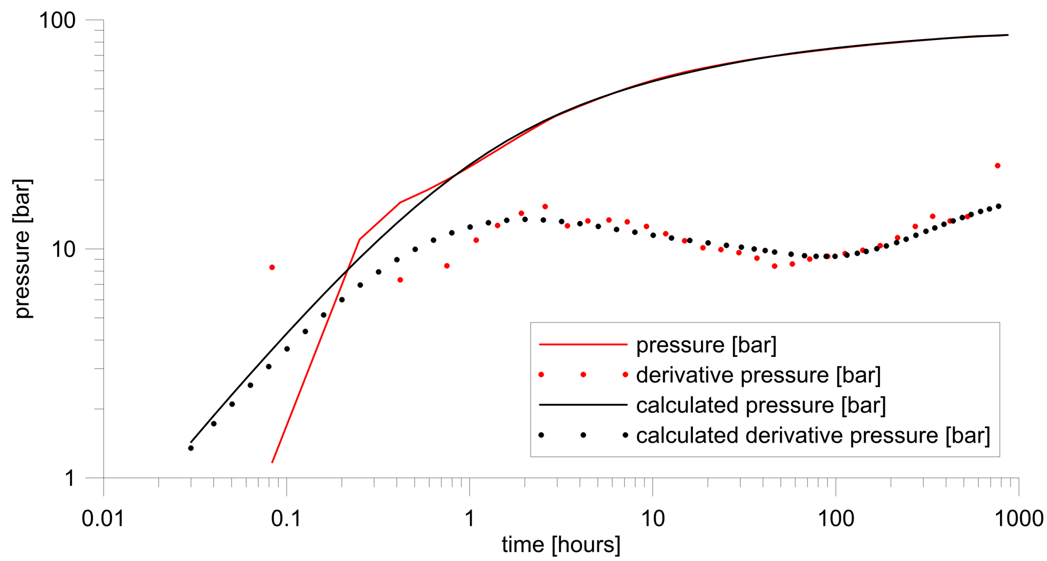

Figure 15: Curve matching of pressure build up and its derivative function as a function of the superposition time for the hydraulic test in April 2012.

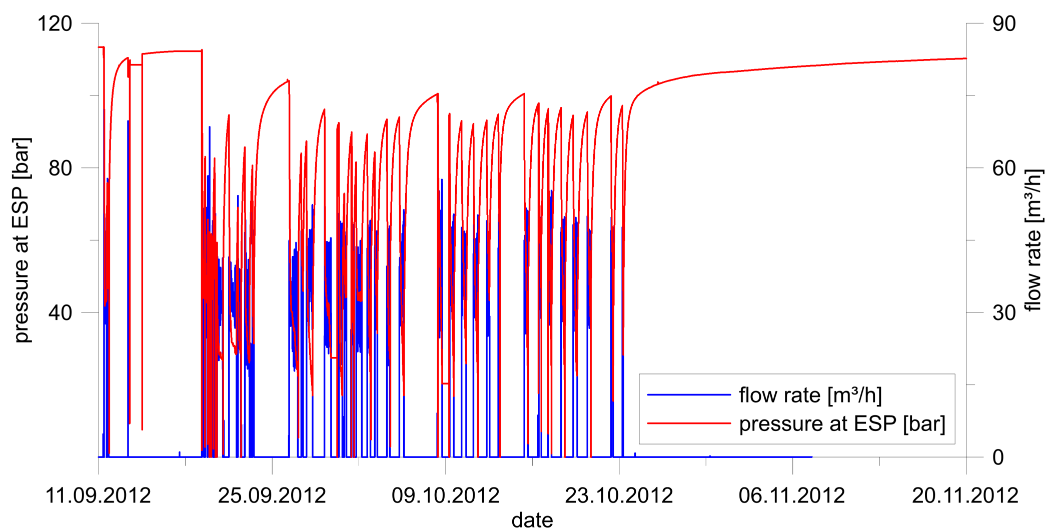

Figure 16: Progression of the hydraulic test in September/October 2012 with additional injection of fresh water.

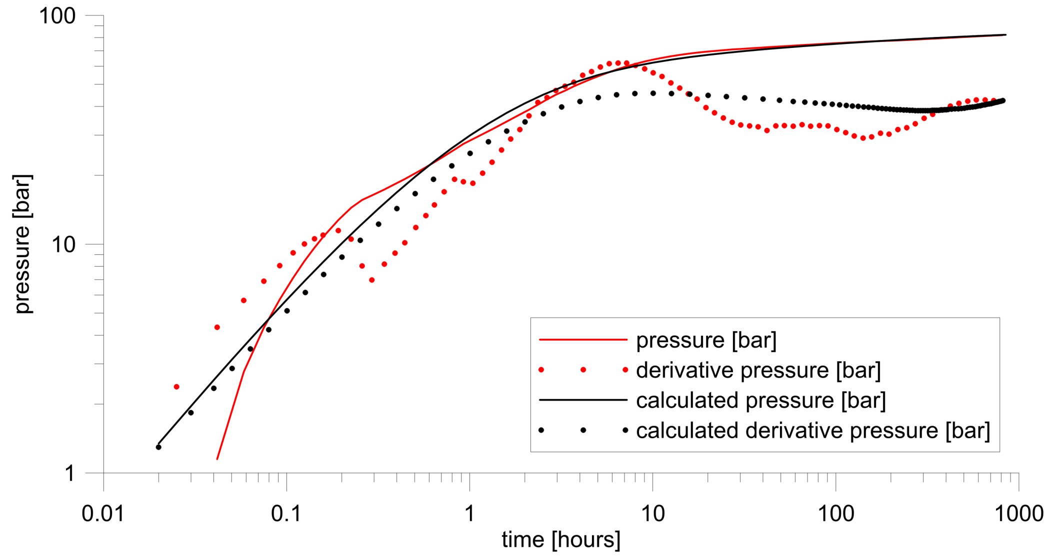

Figure 17: Curve matching of pressure build up and corresponding derivative function for the hydraulic test in September/October 2012.

Table 4: Results of hydraulic test analyses.

	Sept./Oct. 2011	April 2012	Sept./Oct. 2012
Transmissibility [m^3]	$1.24 \cdot 10^{-13}$ m^3	$1.14 \cdot 10^{-13}$ m^3	$8.2 \cdot 10^{-14}$ m^3
Skin [-]	-5.2	-3.7	-5.6
Distance to no-flow boundary [m]	330	122	670
Productivity Index (Standard) [m^3/hMPa]	2.4	1.5	1.9
Productivity Index (Doublet) [m^3/hMPa]	2.1	1.4	1.6